

Solving effective field theory of interacting QCD pomerons in the semi-classical approximation

S. Bondarenko ^{a)}*, L. Motyka ^{b),c)}†

^{a)} *II Institute for Theoretical Physics, University of Hamburg, Germany*

^{b)} *DESY Theory Group, Hamburg, Germany*

^{c)} *Institute of Physics, Jagellonian University, Kraków, Poland*

16 May 2006

Abstract

Effective field theory of BFKL pomerons interacting by QCD triple pomeron vertices is investigated. Classical equations of motion for the effective pomeron fields are presented being a minimal extension of the Balitsky-Kovchegov equation that incorporates both merging and splitting of the pomerons and that is self-dual. The equations are solved for symmetric boundary conditions. The solutions provide the dominant contribution to the scattering amplitudes in the semi-classical approximation. We find that for rapidities of the scattering larger than a critical value Y_c at least two classical solutions exist. Curiously, for each of the two classical solutions with the lowest action the symmetry between the projectile and the target is found to be spontaneously broken, being however preserved for the complete set of classical solutions. The solving configurations at rapidities $Y > Y_c$ consist of a Gribov field being strongly suppressed even at very large gluon momenta and the complementary Gribov field that converges at high Y to a solution of Balitsky-Kovchegov equation. Interpretation of the results is given and possible consequences are shortly discussed.

*Email: sergb@mail.desy.de

†E-mail: motyka@th.if.uj.edu.pl

1 Introduction

Understanding of scattering of hadrons and nuclei at very high energies in terms of Quantum Chromodynamics remains one of the most important challenges for the theory of strong interactions. The reasons for that are both of the phenomenological and of the purely theoretical nature. In practical terms, the basic physics of the present and future colliders, HERA, Tevatron, RHIC and the CERN Large Hadron Collider (LHC), is the physics of high energy scattering in QCD. On the other hand, the high energy regime of QCD reveals intriguing similarities to high energy regime of string theory [1]. To trace and explore postulated dualities between string theories and gauge theories and possible manifestations of those dualities in high energy scattering is a goal of primary importance.

The most successful approach to high energy scattering in QCD is based on infinite resummations of large logarithms of collision energy \sqrt{s} in perturbative expansions of the scattering amplitudes. The corner stone of this formalism is the evolution equation derived by Balitsky, Fadin, Kuraev and Lipatov (BFKL)[2, 3, 4]. In the BFKL framework, the energy evolution of the exchange of an interacting gluon pair in a colour singlet state (the BFKL pomeron) was analyzed at the leading logarithmic (LL) approximation, and consequently, the energy dependence of the hard scattering amplitude was obtained that exhibits a power like growth with energy, $\mathcal{A} \sim s^{1+\Delta}$ with the intercept $\Delta \sim 0.3$. Such behaviour would eventually lead to violation of unitarity. Clearly, this indicates that when the energy is sufficiently large unitarity corrections to the BFKL evolution must be added.

In recent years unitarity effects in high energy QCD have been vigorously investigated along two main lines. The Color Glass Condensate (CGC) approach [5, 6] is formulated in the transverse position space and it is based on energy evolution of Wilson loops and phenomena of rescattering and recombination. In the large N_c limit, the dynamics of the Color Glass Condensate may be analyzed in terms of a statistical model of color dipoles [7]. At a very general level, the dipole description of high energy scattering may be presented as a combination of multiple dipole splittings, the rescattering of dipoles off a target and a stochastic fluctuation term [8].

The QCD Reggeon Field Theory (QCD-RFT) approach is formulated in momentum space and bases the on standard diagrammatic calculus [9, 10, 11, 12, 13, 14]. The main building blocks here are QCD reggeon Green's functions and multi-reggeon vertices derived in the perturbative QCD. Scattering amplitudes may be represented in terms of Feynman diagrams of effective (non-local) reggeon fields. This effective field theory is constructed using the so-called Extended Generalized Leading Logarithmic Approximation (EGLLA) [11] which resums the leading powers of $\alpha_s \log s$ for given topology of the reggeon diagram. The CGC and the QCD-RFT formulations should be, in fact, two different descriptions of the same theory, and they should be equivalent.

In parallel to the theoretical efforts to determine the deep fundamental structure of the effective field theory for high energy scattering, more phenomenological studies of the unitarity effects have been carried out. Probably, a pair of the most fruitful (and entangled) concepts of the last decade were the Balitsky-Kovchegov (BK) evolution equation [5, 15, 16], and the saturation model proposed by Golec-Biernat and Wüsthoff (GBW) [17, 18]. The BK equation was derived in the CGC formulation and in the framework

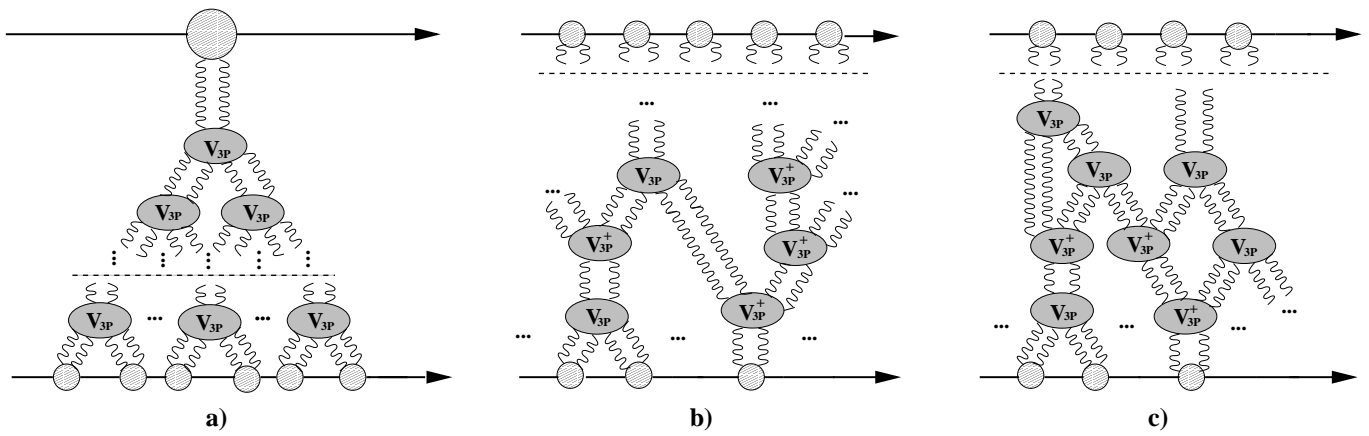


Figure 1: *Examples of diagrams of the effective field theory of QCD pomerons interacting with triple pomeron vertices: a) a fan diagram; b) a tree diagram defining the classical limit; c) a diagram with quantum loops.*

of QCD-RFT it can be viewed as a resummation of the BFKL pomeron fan diagrams of the type depicted in Fig. 1a. An important feature of the BK equation is its simplicity – absence of the vertex for pomeron splitting removes all quantum loops of the complete theory. Therefore, a classical treatment of PFT is exact in the case of the BK equation.

Numerous explicit solutions [19, 20, 21] and semi-analytical analyzes of the BK equation were presented [19, 22, 23] and applications were developed for the deep inelastic scattering (DIS) of nuclei and off the nucleon [24, 25, 26]. Probably, the most remarkable features of the BK equation is generation of the *saturation scale* $Q_s(y)$, increasing exponentially with the available rapidity y : $Q_s(y) \sim \exp(\lambda y)$, and the *geometric scaling* [27, 28, 29]. Both the features of the BK equation are strongly favoured by the experimental data for $\sigma(\gamma^*(Q^2)p)$ down to $Q^2 = 0$, the diffractive DIS data and heavy flavour electroproduction [17, 18, 30]; two-photon cross sections [31]; exclusive photo- and electroproduction of vector mesons and the deeply virtual Compton scattering [32, 33], etc.

Unfortunately, the BK equation is not sufficient to address the problem of scattering of two similar objects, that is the symmetric situation, like proton-proton and nucleus-nucleus collisions at RHIC and the LHC. At present, efforts are made to understand the effective PFT beyond the BK limit [8, 34, 35, 36, 37, 38]. The first key step is to determine properties of the theory after the vertex describing splitting of the pomeron to two pomerons is added to the BK framework. Importantly, the form of this vertex is imposed by the form of the vertex for two pomeron merging. The reason for that is that the two vertices differ only by the choice of direction of evolution in rapidity, which is arbitrary and should have no impact on physics. This simple fact was known in the RFT since a long time [39, 40, 41] and recently it was re-discovered in the CGC framework, as the self-duality of the CGC Hamiltonian [42]. With the pomeron splitting vertex quantum pomeron loops become possible, as exemplified in Fig. 1c, and solving the theory becomes much more difficult. There exists, however, an interesting limit in which some explicit results can be found. Namely, collision of two large nuclei composed of $A \gg 1$ nucleons each, can be analyzed. In the limit of very large A the quantum pomeron loops will provide only subleading contribution, suppressed by powers $1/A$. Then, the tree topologies of the pomeron diagrams give the dominant contribution to the S -matrix,

corresponding to the classical limit of the effective Pomeron Field Theory. A pomeron diagram that has the tree topology is shown in Fig. 1b. This concept was put forward and developed in a series of pioneering papers by Braun [34, 35, 36], and an analogous path was taken by Balitsky in the framework of the Color Glass Condensate [38]. In the present study we provide a complementary analysis to that of Braun, solving the classical equations of motion of the Pomeron Field Theory, and reporting observations of some new, unexpected features of the PFT. Among them, perhaps, the most surprising is a break-down of the symmetry between the target and the projectile at the classical level.

The paper is organized as follows. In the next section we describe the formalism of the effective QCD Pomeron Field Theory. In Sec. 3 we provide insight into the theory coming from a toy model of the Reggeon Field Theory in zero transverse dimensions. In Sec. 4 solutions of PFT are presented. We discuss the results in Sec. 5 and conclude in Sec. 6.

2 Formalism

2.1 The Balitsky-Kovchegov equation and the triple pomeron vertex

Scattering of the small perturbative probe off a large nucleus was studied by Balitsky and Kovchegov [5, 15, 16]. Balitsky derived the rapidity evolution equations describing the scattering amplitude in QCD, which involved an infinite tower of the correlators. This hierarchy is cut down to the lowest correlator in the large N_c limit, leading to a much simpler and better tractable evolution equation. Such an equation was derived by Kovchegov in the framework of the dipole model. Thus, the Balitsky-Kovchegov equation provides the correct limit of the scattering amplitude in QCD for a large nucleus at the LLs accuracy, and for $1/N_c \rightarrow 0$. In the infinite momentum frame, the BK equation resums the BFKL pomeron fan diagrams (see Fig. 1a), with the triple pomeron vertex equivalent to the Bartels vertex at the leading $1/N_c$ accuracy.

The BK equation was initially proposed as a non-linear evolution equation for the dipole scattering amplitude $N(y; \mathbf{r}, \mathbf{b})$, where the dipole spans the vector \mathbf{r} and is located at the transverse position \mathbf{b} . Thus, the BK equation reads

$$\begin{aligned} \frac{\partial N(y; \mathbf{r}, \mathbf{b})}{\partial y} &= \bar{\alpha}_s (\tilde{\mathcal{K}} \otimes N)(y; \mathbf{r}, \mathbf{b}) \\ &- \bar{\alpha}_s \int \frac{d^2 \mathbf{r}'}{2\pi} \frac{r^2}{r'^2 (\mathbf{r} + \mathbf{r}')^2} N\left(y; \mathbf{r} + \mathbf{r}', \mathbf{b} + \frac{\mathbf{r}'}{2}\right) N\left(y; \mathbf{r}', \mathbf{b} + \frac{\mathbf{r} + \mathbf{r}'}{2}\right). \end{aligned} \quad (1)$$

where $\bar{\alpha}_s = N_c \alpha_s / \pi$, and the linear term is determined by the BFKL kernel in the position space

$$(\tilde{\mathcal{K}} \otimes N)(y; \mathbf{r}, \mathbf{b}) = \int \frac{d^2 \mathbf{r}'}{2\pi r'^2} \left\{ \frac{2r^2}{(\mathbf{r} + \mathbf{r}')^2} N(y; \mathbf{r} + \mathbf{r}', \mathbf{b}) - \frac{r^2}{r'^2 + (\mathbf{r} + \mathbf{r}')^2} N(y; \mathbf{r}, \mathbf{b}) \right\}. \quad (2)$$

In the limit of the small scattering amplitude the quadratic term may be neglected and the BFKL equation in the dipole picture is obtained.

The BK equation is a differentio-integral equation, for which the integral kernel depends on two two-dimensional vectors \mathbf{r} and \mathbf{b} . Numerical solution of the complete equation is possible [20] but cumbersome.

Besides that, the treatment of the large dipoles and large impact parameters in the BK equation is, strictly speaking, incorrect as far as QCD is concerned. Namely, the confinement of colour is not accounted for, which can be seen, for instance from the conformal invariance of the equation. Thus, the Froissart limit for the scattering matrix is broken due to a power like diffusion to the large impact parameters [43]. Thus, in this work we follow the approximation made in the earlier analyzes that the dominant contribution to the scattering amplitude comes from perturbative dipoles for which $r \ll R$, where R is the nucleus size. In this case the evolution may be assumed to be local in the transverse plane and Eq. (1) becomes independent of \mathbf{b} . Thus, the \mathbf{b} -dependence can be suppressed in $N(y; \mathbf{r}, \mathbf{b})$ and it enters only through the initial condition for the evolution equation.

For an azimuthally symmetric solution, $N(y, \mathbf{r}) = N(y, r)$, it is convenient to Fourier transform Eq. (1) to the momentum space,

$$\phi(k^2, y) = \int \frac{d^2 \mathbf{r}}{2\pi} \exp(-i\mathbf{k} \cdot \mathbf{r}) \frac{N(y, r)}{r^2} = \int_0^\infty \frac{dr}{r} J_0(kr) N(y, r), \quad (3)$$

where J_0 is the Bessel function. In this case the following equation is obtained

$$\frac{\partial \phi(y, k^2)}{\partial y} = \bar{\alpha}_s (\mathcal{K}' \otimes \phi)(y, k^2) - \bar{\alpha}_s \phi^2(y, k^2), \quad (4)$$

and the action of the BFKL kernel (suitably shifted in the space of the Mellin moments in k^2) is given by

$$(\mathcal{K}' \otimes \phi)(y, k^2) = \int_0^\infty \frac{da^2}{a^2} \left\{ \frac{a^2 \phi(y, a^2) - k^2 \phi(y, k^2)}{|k^2 - a^2|} + \frac{k^2 \phi(y, k^2)}{\sqrt{4a^4 + k^4}} \right\}, \quad (5)$$

where k^2 and a^2 are the virtualities of the exchanged gluons in the BFKL ladder.

Equation (4) may be further transformed to the form dependent on the unintegrated gluon density in the transverse space [25]. One has

$$f(y, k^2) = \frac{N_c}{4\alpha_s \pi^2} k^4 \nabla_k^2 \phi(y, k^2), \quad (6)$$

and conversely,

$$\phi(y, k^2) = \frac{\pi^2 \alpha_s}{N_c} \int_{k^2} \frac{da^2}{a^4} f(y, a^2) \log \left(\frac{a^2}{k^2} \right). \quad (7)$$

The unintegrated gluon density in the transverse space may be related in the small- x limit to the collinear gluon distribution of the target A

$$\int_A d^2 \mathbf{b} f(y, k^2, \mathbf{b}) = \frac{\partial x g(x, k^2)}{\partial \log k^2}, \quad (8)$$

where $y = \log(1/x)$ and we restored the dependence of $f(y, k^2, \mathbf{b})$ on the transverse position \mathbf{b} , assuming that it is mild enough to ensure effective decoupling of the \mathbf{b} dependence from the BK evolution, which should hold for a large target.

After this transform is executed the BK equation reads [25]

$$\partial_y f(y, k^2) = \frac{N_c \alpha_s}{\pi} k^2 \int \frac{da^2}{a^2} \left[\frac{f(a^2) - f(k^2)}{|a^2 - k^2|} + \frac{f(k^2)}{[4a^4 + k^4]^{\frac{1}{2}}} \right]$$

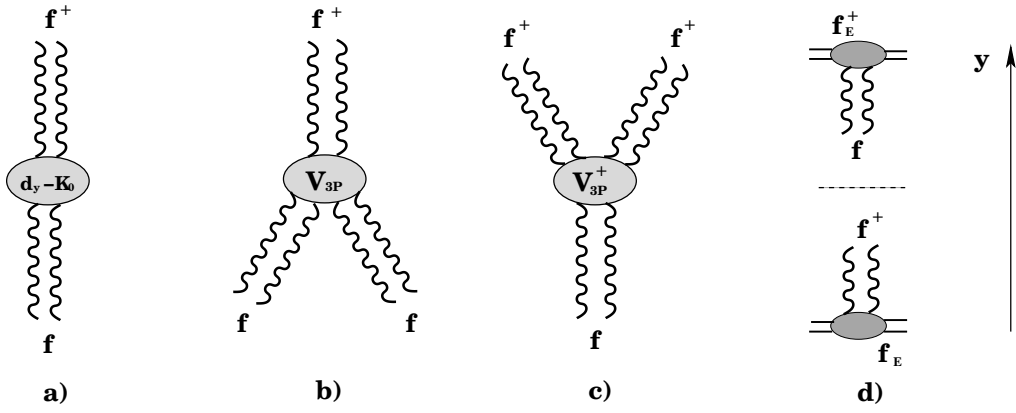


Figure 2: *Elements of the effective action: a) the BFKL pomeron propagator; b) the merging vertex; c) the splitting vertex and d) the external sources of the fields. The arrow indicates the direction of evolution.*

$$- 2\pi\alpha_s^2 \left[k^2 \int_{k^2} \frac{da^2}{a^4} f(y, a^2) \int_{k^2} \frac{db^2}{b^4} f(y, b^2) + f(y, k^2) \int_{k^2} \frac{da^2}{a^4} \log \left(\frac{a^2}{k^2} \right) f(y, a^2) \right]. \quad (9)$$

It is easy to verify that the nonlinear term describing joining of two pomerons, $(f, f) \rightarrow f$ is generated from the amplitude of the Bartels triple pomeron vertex (in the forward limit),

$$\begin{aligned} (f^\dagger | V_{3P} | f \otimes f) &= -2\pi\alpha_s^2 \int \frac{da^2}{a^4} a^2 f^\dagger(y, a^2) \int_{a^2} \frac{db^2}{b^4} f(y, b^2) \int_{a^2} \frac{dc^2}{c^4} f(y, c^2) \\ &\quad - 2\pi\alpha_s^2 \int \frac{da^2}{a^4} f^\dagger(y, a^2) f(y, a^2) \int_{a^2} \frac{db^2}{b^4} \log \left(\frac{b^2}{a^2} \right) f(y, b^2). \end{aligned} \quad (10)$$

by functional differentiation with respect to the pomeron field $f^\dagger(y, k^2)$. The details of the complete effective action for interacting pomerons are given in the next section.

2.2 Effective action and the self-duality

Following Braun [34, 35, 36], we shall construct an effective action to represent both pomeron merging and splitting. We wish to study the minimal extension of the BK equation, thus we neglect vertices at which more than three pomerons meet. It is clear that the vertex for pomeron splitting must be the same as the vertex for pomeron merging. The reason is that in order to distinguish merging of the pomerons from a splitting of a pomeron we have to specify the direction of the evolution in rapidity. This choice is, however, completely arbitrary and the form the action should not depend on it. More precisely, the inversion of the direction of evolution, $y \rightarrow -y$ results with the interchange of the outgoing (f^\dagger) and incoming (f) pomeron fields. In result, the effective action is invariant under the transform,

$$f \leftrightarrow f^\dagger, \quad y \rightarrow -y, \quad (11)$$

and the form of the splitting vertex $(f^\dagger \otimes f^\dagger | V_{3P}^\dagger | f)$ is given by $(f^\dagger | V_{3P} | f \otimes f)^\dagger$.

Thus, in what follows we shall write the effective action for the interacting pomeron system based on the following principles:

1. Free propagation of the pomeron fields is described by the forward BFKL equation.
2. Pomerons interact only through triple pomeron vertices.
3. The vertex for merging of the pomerons is the Bartels triple pomeron vertex at large N_c and in the forward limit, equivalent to the vertex that generates the Balitsky-Kovchegov equation.
4. Splitting and merging of the pomerons are described by identical vertices.
5. The fields do not depend on the transverse position.

The elements of the action are graphically represented in Fig. 2. The above assumptions lead to a unique form of the action,

$$\mathcal{A}[f, f^\dagger; Y] = \frac{4\pi^3}{N_c^2 - 1} \int_0^Y dy \left\{ \mathcal{L}_0[f, f^\dagger] + \mathcal{L}_3[f, f^\dagger] + \mathcal{L}_3^\dagger[f, f^\dagger] + \mathcal{L}_E[f, f^\dagger] \right\}, \quad (12)$$

where the Lagrange function for the free propagation reads

$$\begin{aligned} \mathcal{L}_0[f, f^\dagger] &= \frac{1}{2} \int \frac{da^2}{a^4} \left[f(y, a^2) \partial_y f^\dagger(y, a^2) - f^\dagger(y, a^2) \partial_y f(y, a^2) \right] \\ &\quad + \int \frac{da^2}{a^4} \int \frac{db^2}{b^4} f^\dagger(y, a^2) \mathcal{K}_0(a^2, b^2) f(y, b^2), \end{aligned} \quad (13)$$

and \mathcal{K}_0 is the amputated forward BFKL kernel given by

$$\int \frac{db^2}{b^4} \mathcal{K}_0(a^2, b^2) f(b^2) = \frac{N_c \alpha_s}{\pi} a^2 \int \frac{db^2}{b^2} \left[\frac{f(b^2) - f(a^2)}{|b^2 - a^2|} + \frac{f(a^2)}{[4b^4 + a^4]^{\frac{1}{2}}} \right]. \quad (14)$$

The Lagrange function describing merging of two pomerons takes the form

$$\begin{aligned} \mathcal{L}_3[f, f^\dagger] &= -2\pi\alpha_s^2 \int \frac{da^2}{a^4} a^2 f^\dagger(y, a^2) \int_{a^2} \frac{db^2}{b^4} f(y, b^2) \int_{a^2} \frac{dc^2}{c^4} f(y, c^2) \\ &\quad - 2\pi\alpha_s^2 \int \frac{da^2}{a^4} f^\dagger(y, a^2) f(y, a^2) \int_{a^2} \frac{db^2}{b^4} \log\left(\frac{b^2}{a^2}\right) f(y, b^2). \end{aligned} \quad (15)$$

Splitting of a pomeron contributes with

$$\begin{aligned} \mathcal{L}_3^\dagger[f, f^\dagger] &= -2\pi\alpha_s^2 \int \frac{da^2}{a^4} a^2 f(y, a^2) \int_{a^2} \frac{db^2}{b^4} f^\dagger(y, b^2) \int_{a^2} \frac{dc^2}{c^4} f^\dagger(y, c^2) \\ &\quad - 2\pi\alpha_s^2 \int \frac{da^2}{a^4} f(y, a^2) f^\dagger(y, a^2) \int_{a^2} \frac{db^2}{b^4} \log\left(\frac{b^2}{a^2}\right) f^\dagger(y, b^2). \end{aligned} \quad (16)$$

The coupling of the pomerons to the external sources is represented by

$$\mathcal{L}_E[f, f^\dagger] = \int \frac{da^2}{a^4} \left[f_E^\dagger(y, a^2) f(y, a^2) + f^\dagger(y, a^2) f_E(y, a^2) \right], \quad (17)$$

where the external sources will be assumed to be localized in rapidity,

$$f_E(y, a^2) = f_A(a^2) \delta(y), \quad f_E^\dagger(y, a^2) = f_B^\dagger(a^2) \delta(y - Y). \quad (18)$$

Clearly, f_A represents the amplitude of emission of the pomeron described by the field $f(y, k^2)$ from the source at $y = 0$ and f_B^\dagger is the coupling of $f^\dagger(y, k^2)$ to an external source at $y = Y$.

Let us stress that the treatment of the transverse position is missing and thus the evaluation of the quantum loops of the complete theory cannot be performed with this action. Nevertheless, the action treated in the semi-classical framework may be used to approximately resum the BFKL pomeron tree diagrams (see Fig. 1b) in scattering of two large objects, for instance of two nuclei. For a scattering in which the projectile and the target have sizes much larger than the typical momenta in the QCD pomeron, the momentum transfer of the pomeron line originating from the external particles is bounded to be small by the form-factors of the sources and may be therefore neglected. In the diagrams without closed pomeron loops the constraint imposed on momentum transfer of the external lines propagates and extends to all pomeron lines.

In fact, a complete action that properly represents the degrees of freedom corresponding to the momentum transfer (or equivalently to the transverse positions of the pomerons), that are missing in the action (12), was proposed by Braun [36]. It is also straightforward to write down an analogous action in the present formulation. That complete action, however, leads to the same dynamics of a scattering of two large objects in the semi-classical limit, the problem that we address in this work. Therefore, we restrict ourselves to the simplified effective action given by (12).

Let us return to the symmetry of the action defined by Eq. (11). This symmetry causes the action to be self-dual. Indeed, after integration by parts of the “time derivative” part of the action

$$\int_0^Y dy \frac{1}{2} \left[f(y, a^2) \partial_y f^\dagger(y, a^2) - f^\dagger(y, a^2) \partial_y f(y, a^2) \right] \rightarrow \int_0^Y dy \left[-f^\dagger(y, a^2) \partial_y f(y, a^2) \right] + (\dots) \quad (19)$$

where (\dots) denote the boundary terms, one gets that

$$\frac{\delta \mathcal{L}[f, f^\dagger]}{\delta(\partial_y f(y, k^2))} = -\frac{1}{k^4} f^\dagger(y, k^2). \quad (20)$$

This means, that the field $f^\dagger(y, k^2)$ is the canonical conjugate of $f(y, k^2)$, up to the factor of $1/k^4$ which can be easily absorbed into the field definitions and trivial complex phase factors. After invoking the symmetry (11) we conclude that the bulk part of the action (12) may be rewritten in the self-dual form. The symmetry of the action (12) may be completed by assuming the symmetric external sources, that enter \mathcal{L}_E . Then, one expects the solution of the field equations $\{f, f^\dagger\}$ to be also symmetric

$$f(y, k^2) = f^\dagger(Y - y, k^2). \quad (21)$$

In what follows, we shall refer to this as to the *projectile-target symmetry*.

2.3 Equations of motion

Let us list the functional derivatives of the action of the effective Pomeron Field Theory (12) with respect to $f^\dagger(y, k^2)$:

$$\frac{\delta \mathcal{L}_0[f, f^\dagger]}{\delta(\partial_y f^\dagger(y, k^2))} = \frac{1}{2} \frac{1}{k^4} f(y, k^2); \quad (22)$$

$$\frac{\delta \mathcal{L}_0[f, f^\dagger]}{\delta f^\dagger(y, k^2)} = -\frac{1}{k^4} \left[\frac{1}{2} \partial_y f(y, k^2) - \int \frac{db^2}{b^4} \mathcal{K}_0(k^2, b^2) f(y, b^2) \right]; \quad (23)$$

$$\frac{\delta \mathcal{L}_3[f, f^\dagger]}{\delta f^\dagger(y, k^2)} = -2\pi\alpha_s^2 \frac{1}{k^4} \left[k^2 \int_{k^2} \frac{da^2}{a^4} f(y, a^2) \int_{k^2} \frac{db^2}{b^4} f(y, b^2) + f(y, k^2) \int_{k^2} \frac{da^2}{a^4} \log\left(\frac{a^2}{k^2}\right) f(y, a^2) \right]; \quad (24)$$

$$\begin{aligned} \frac{\delta \mathcal{L}_3^\dagger[f, f^\dagger]}{\delta f^\dagger(y, k^2)} = & -2\pi\alpha_s^2 \frac{1}{k^4} \left[2 \int_0^{k^2} \frac{da^2}{a^4} a^2 f(y, a^2) \int_{a^2} \frac{db^2}{b^4} f^\dagger(y, b^2) \right. \\ & \left. + f(y, k^2) \int_{k^2} \frac{da^2}{a^4} \log\left(\frac{a^2}{k^2}\right) f^\dagger(y, a^2) + \int_0^{k^2} \frac{da^2}{a^4} f(y, a^2) f^\dagger(y, a^2) \log\left(\frac{k^2}{a^2}\right) \right]; \end{aligned} \quad (25)$$

$$\frac{\delta \mathcal{L}_E[f, f^\dagger]}{\delta f^\dagger(y, k^2)} = \frac{1}{k^4} f_E(y, k^2). \quad (26)$$

Analogously one computes the functional derivatives with respect to $f(y, k^2)$. The results of that procedure may be obtained by an interchange of $f \leftrightarrow f^\dagger$ in equations (22–26) and changing the sign of $f(y, k^2)$ in (22) and of the $\partial_y f(y, k^2)$ in (23). Thus, one obtains the following equations of motion,

$$\begin{aligned} \partial_y f(y, k^2) = & \frac{N_c \alpha_s}{\pi} k^2 \int \frac{da^2}{a^2} \left[\frac{f(a^2) - f(k^2)}{|a^2 - k^2|} + \frac{f(k^2)}{[4a^4 + k^4]^{\frac{1}{2}}} \right] \\ & - 2\pi\alpha_s^2 \left[k^2 \int_{k^2} \frac{da^2}{a^4} f(y, a^2) \int_{k^2} \frac{db^2}{b^4} f(y, b^2) + f(y, k^2) \int_{k^2} \frac{da^2}{a^4} \log\left(\frac{a^2}{k^2}\right) f(y, a^2) \right] \\ & - 2\pi\alpha_s^2 \left[2 \int_0^{k^2} \frac{da^2}{a^4} a^2 f(y, a^2) \int_{a^2} \frac{db^2}{b^4} f^\dagger(y, b^2) + f(y, k^2) \int_{k^2} \frac{da^2}{a^4} \log\left(\frac{a^2}{k^2}\right) f^\dagger(y, a^2) \right] \\ & - 2\pi\alpha_s^2 \int_0^{k^2} \frac{da^2}{a^4} f(y, a^2) f^\dagger(y, a^2) \log\left(\frac{k^2}{a^2}\right), \end{aligned} \quad (27)$$

and

$$\begin{aligned} -\partial_y f^\dagger(y, k^2) = & \frac{N_c \alpha_s}{\pi} k^2 \int \frac{da^2}{a^2} \left[\frac{f^\dagger(a^2) - f^\dagger(k^2)}{|a^2 - k^2|} + \frac{f^\dagger(k^2)}{[4a^4 + k^4]^{\frac{1}{2}}} \right] \\ & - 2\pi\alpha_s^2 \left[k^2 \int_{k^2} \frac{da^2}{a^4} f^\dagger(y, a^2) \int_{k^2} \frac{db^2}{b^4} f^\dagger(y, b^2) + f^\dagger(y, k^2) \int_{k^2} \frac{da^2}{a^4} \log\left(\frac{a^2}{k^2}\right) f^\dagger(y, a^2) \right] \\ & - 2\pi\alpha_s^2 \left[2 \int_0^{k^2} \frac{da^2}{a^4} a^2 f^\dagger(y, a^2) \int_{a^2} \frac{db^2}{b^4} f(y, b^2) + f^\dagger(y, k^2) \int_{k^2} \frac{da^2}{a^4} \log\left(\frac{a^2}{k^2}\right) f(y, a^2) \right] \\ & - 2\pi\alpha_s^2 \int_0^{k^2} \frac{da^2}{a^4} f^\dagger(y, a^2) f(y, a^2) \log\left(\frac{k^2}{a^2}\right), \end{aligned} \quad (28)$$

with the two-point boundary conditions,

$$f(y=0, k^2) = f_A(k^2), \quad f^\dagger(y=Y, k^2) = f_B^\dagger(k^2). \quad (29)$$

The equations are equivalent to the equations derived by Braun [34], although they are formulated using other variables. Therefore we shall refer to equations (27), (28) as to the *Braun equations*. Apparently, the present formulation is more complicated and less convenient than the original one. Still, it might be advantageous to use the present form. The reason is that the interpretation of the degrees of freedom that we use is straightforward in terms of perturbative QCD in the momentum space; the basic physical objects: the unintegrated gluon and the triple pomeron vertex in the momentum space are represented in a transparent way. Using the present form it should be also relatively simple to account for non-leading corrections to the BFKL kernel, as it was done for the BK equation [25].

2.4 The S -matrix

Solutions to classical equations of motions for the pomeron fields may be used to determine the S -matrix for the high energy scattering in the semi-classical approximation. In order to do that, however, the dependence of the problem on the transverse position has to be taken into account.

First, let us consider the general case, in which the action has the complete dependence on the transverse position. Thus, the pomeron fields depend on the position \mathbf{b}_1 and \mathbf{b}_2 with respect to the center of the projectile and the target, correspondingly: $f(y, k^2) \rightarrow \tilde{f}(y, k^2, \mathbf{b}_1)$ and $f^\dagger(y, k^2) \rightarrow \tilde{f}^\dagger(y, k^2, \mathbf{b}_2)$. Suppose that we know the solutions to the Braun equations with the full dependence of the transverse position for a given impact parameter \mathbf{b} of the collision. Then, the complete action may be evaluated for such a solution by performing integrations over transverse positions of all the fields, with the weights provided by the \mathbf{b} -dependent Lagrangian density.

In this paper we do not attempt to resolve the complex dynamics of the fields in the transverse plane. Therefore we should apply an approximate treatment, in the spirit of the original work of Kovchegov and following the initial Braun proposal. Those authors assumed that the sources of pomeron fields were large nuclei. Those objects are much larger than typical pomeron sizes, defined as inverse of the typical gluon virtualities in the pomeron. Therefore, for the bulk of interactions, an approximate translational invariance in the transverse space holds. This is not true only at the nucleus boundary, which gives, however, only a subleading contribution to the scattering amplitude. The simplest way to approximately account for this situation is to assume that the action is local in the transverse position. Then, it is enough to solve the Braun equations with input conditions dependent on the transverse position, $\tilde{f}_A(k^2, \mathbf{b}_1)$ and $\tilde{f}_B^\dagger(k^2, \mathbf{b}_1 - \mathbf{b})$ at given impact parameter vector \mathbf{b} . In writing so, we assume that the initial condition $\tilde{f}_A(k^2, \mathbf{b}_1)$ is centered at $b_1 = 0$ and the distribution $\tilde{f}_B^\dagger(k^2, \mathbf{b}_1 - \mathbf{b})$ develops around the point whose position is given by \mathbf{b} . For instance, for a collision of two cylindrical nuclei with the same radius R , one has: $\tilde{f}_A(k^2, \mathbf{b}_1) = f_A(k^2)\Theta(R - b_1)$ and $\tilde{f}_B^\dagger(k^2, \mathbf{b}_2) = f_B^\dagger(k^2)\Theta(R - b_2)$.

Thus, assuming locality of the evolution in the transverse space the complete action takes the form

$$\tilde{\mathcal{A}}[\tilde{f}, \tilde{f}^\dagger; Y, \mathbf{b}] = \int d^2\mathbf{b}_1 \mathcal{A}[\tilde{f}(y, k^2, \mathbf{b}_1), \tilde{f}^\dagger(y, k^2, \mathbf{b} - \mathbf{b}_1); Y], \quad (30)$$

where the equations of motion may be employed to obtain

$$\mathcal{A}[\tilde{f}, \tilde{f}^\dagger; Y] = \frac{1}{2} \int_{0-}^{Y+} dy \left\{ \mathcal{L}_E[\tilde{f}, \tilde{f}^\dagger] - \mathcal{L}_3[\tilde{f}, \tilde{f}^\dagger] - \mathcal{L}_3^\dagger[\tilde{f}, \tilde{f}^\dagger] \right\}, \quad (31)$$

leading, in the semi-classical approximation, to the S -matrix

$$S(Y, \mathbf{b}) = \exp\{-\tilde{\mathcal{A}}[\tilde{f}, \tilde{f}^\dagger; Y, \mathbf{b}]\}. \quad (32)$$

Some more details and subtleties of this approximation will be discussed in the next section.

3 Toy model – Reggeon Field Theory in zero transverse dimensions

3.1 Formulation

As a constructive example of a possible qualitative behavior of the interacting pomeron system we consider a zero dimensional toy model of interacting pomerons, the, so called, Reggeon Field Theory in zero transverse dimensions (RFT-0). The model of RFT-0 was formulated and studied in depth long time ago, see e.g. [39, 40] and recently it has enjoyed a revived interest [44, 45]. In fact, it turns out that RFT-0 in the weak coupling regime exhibits some generic features which seem to be present also for interacting QCD pomerons. Therefore, this much simpler model may be used to provide some insight into the complex dynamics of QCD Pomeron Field Theory.

This model is determined by the action

$$\mathcal{A}_{\text{RFT-0}}[q(y), p(y); Y] = \int_0^Y dy \mathcal{L}_{\text{RFT-0}}. \quad (33)$$

with the Lagrangian:

$$\mathcal{L}_{\text{RFT-0}} = \frac{1}{2} q \partial_y p - \frac{1}{2} p \partial_y q + \mu q p - \lambda q (q + p) p + p(y) q_0(y) + p_0(y) q(y), \quad (34)$$

where μ is the intercept of the pomeron, λ is the triple pomeron coupling and $\{q, p\}$ are (up to complex phase factors) Gribov fields depending only on rapidity and responsible for the creation and annihilations of pomerons. They correspond to f and f^\dagger of the BFKL Pomeron Field Theory. The functions $q_0(y)$ and $p_0(y)$ are the external sources of the q and p fields respectively. In analogy to the assumptions of the previous section we shall consider a scattering process at rapidity Y with the source terms assumed to take the form:

$$q_0(y) = g_1 \delta(y), \quad p_0(y) = g_2 \delta(y - Y). \quad (35)$$

Note, that the action is invariant under the duality transformation

$$p \leftrightarrow q \quad \text{and} \quad y \rightarrow Y - y \quad (36)$$

for symmetric boundary conditions $g_1 = g_2$ (obviously, the bulk action is invariant for any external couplings).

Dynamics of the system defined by the Lagrangian (34) was intensively investigated both in the complete quantum framework [40] and in the semi-classical approximation [39]. Here, we focus on the latter treatment in order to match the approximations which we use in the description of the BFKL Pomeron Field Theory.

Thus, the quantum evolution of the system may be represented by the S -matrix expressed using the path integral

$$S(Y; g_1, g_2) = \int [Dq Dp] \exp \{ -\mathcal{A}_{RFT-0}[q(y), p(y); Y] \}, \quad (37)$$

where the probe trajectories obey $q(0) = 0$ and $p(Y) = 0$, as the initial conditions are absorbed in the action. In the semi-classical limit, the dominant contribution to the path integral comes from the classical trajectories $\{\bar{q}_\alpha, \bar{p}_\alpha\}$ for which the action is stationary,

$$S(Y; g_1, g_2) \simeq \sum_\alpha \Delta_\alpha \exp \{ -\mathcal{A}_{RFT-0}[\bar{q}_\alpha, \bar{p}_\alpha; Y] \}, \quad (38)$$

where Δ_α represent the quantum weights of subsequent classical trajectories, which at the leading approximation come from resummation of Gaussian quantum fluctuations around the classical trajectory. Note, that the system evolves in rapidity which is formally equivalent to an evolution in the Euclidean time, thus the S -matrix is dominated by classical trajectories with the minimal value of the action. It is important to stress that the action of RFT-0 exhibits the feature of self-duality (or projectile-target symmetry) as its PFT counterpart.

3.2 Solutions: spontaneous breaking of projectile-target symmetry

The extremal value of the action is reached for classical trajectories $\{q, p\}$ which obey the equations of motion,

$$\partial_y q = \mu q - \lambda q^2 - 2\lambda q p \quad (39)$$

$$-\partial_y p = \mu p - \lambda p^2 - 2\lambda q p \quad (40)$$

with the two-side boundary condition

$$q(0) = g_1, \quad p(Y) = g_2. \quad (41)$$

For $g_1 < \mu/\lambda$ and $g_2 < \mu/\lambda$ the classical trajectories are confined to a triangle in the phase space spanned by points with (p, q) coordinates: $(0, 0)$, $(0, \mu/\lambda)$ and $(\mu/\lambda, 0)$. These boundary conditions permit for existence of multiple solutions provided that rapidity Y is large enough. Thus, for Y smaller than a critical value Y_c (depending on g_1 , g_2 , λ and μ) there exists a unique solution to the classical problem, $\{\bar{q}_1(y; g_1, g_2), \bar{p}_1(y; g_1, g_2)\}$. In the case of $g_1 = g_2 = g$ the solution preserves the symmetry between the target and the projectile,

$$\bar{q}_1(y; g, g) = \bar{p}_1(Y - y; g, g). \quad (42)$$

This simple picture changes at $Y = Y_c$. In this point two more solutions $\{\bar{q}_2(y; g, g), \bar{p}_2(y; g, g)\}$ and $\{\bar{q}'_2(y; g, g), \bar{p}'_2(y; g, g)\}$ become possible which do not inherit the symmetry between the target and the projectile embedded in the action and the boundary conditions,

$$\bar{q}_2(y; g, g) \neq \bar{p}_2(Y - y; g, g), \quad \text{and} \quad \bar{q}'_2(y; g, g) \neq \bar{p}'_2(Y - y; g, g). \quad (43)$$

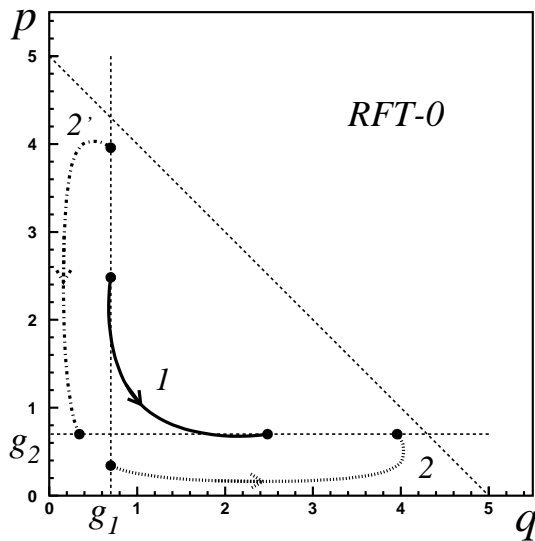


Fig. 3-a

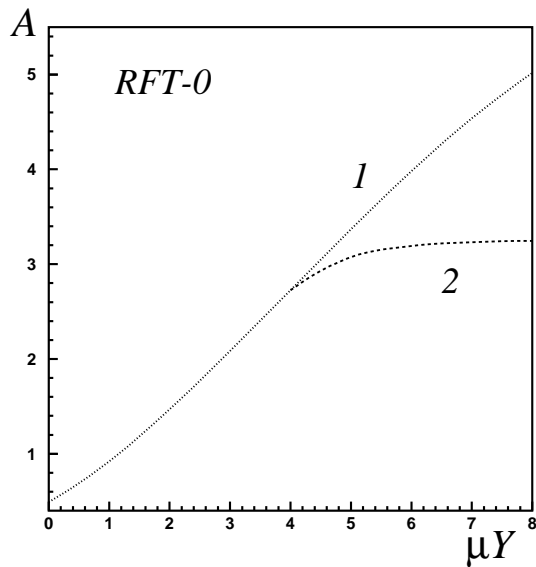


Fig. 3-b

Figure 3: *Classical solutions of the RFT-0: a) the $\{q, p\}$ trajectories for $Y > Y_c$; b) value of the action $\mathcal{A}_{RFT-0}[\bar{q}(y; g, g), \bar{p}(y; g, g); Y]$ for the symmetric solution (dotted line) and the asymmetric solution (dashed line) as a function of scaled rapidity μY .*

An example of the solutions is given in Fig. 3a plotted in the phase space $\{p, q\}$. The parameters of the model were chosen to be $\mu/\lambda = 5$, $g_1 = g_2 = 0.7$, and $\mu Y = 8$. For this rapidity, one finds the symmetric trajectory 1 and two asymmetric trajectories: 2 and 2'. At yet larger values of rapidity Y more solutions are possible, corresponding to cycles in the phase space and giving larger values of the action, so we neglect those cycles in the present analysis.

The value of the action corresponding to trajectories 1 and 2 is plotted in Fig. 3b as a function of the total rescaled rapidity μY . Note, that trajectory 2 is only possible for $Y > Y_c$, and the critical rapidity $Y_c \simeq 4$ for our choice of parameters. Clearly, the value of the action is smaller for the asymmetric trajectories, therefore the asymmetric trajectories are expected to dominate the Euclidean path integral defining the scattering amplitude at large rapidities. At $Y = Y_c$, however, the action of the asymmetric trajectory joins smoothly the action of the symmetric trajectory. Thus, one concludes that at the transition region of $Y \simeq Y_c$ the contribution of trajectory 1 to the scattering amplitude should be also included.

Note, that the emergence of the dominant asymmetric solutions may be interpreted in terms of *spontaneous breaking of a discrete symmetry* of the action. The symmetry between the projectile and the target (leading to the self-duality of the action) is built in the action (33) and in the boundary conditions. Clearly, this is a discrete symmetry. The dominant solutions of the equations of motion, however, are not symmetric. Thus, the symmetry is spontaneously broken. This is possible, as the boundary conditions are defined at two points of rapidity and the classical solutions need not be unique. As usual, however, the symmetry still holds for the full set of solutions,

$$\bar{q}'_2(y; g, g) = \bar{p}_2(Y - y; g, g) \quad \text{and} \quad \bar{p}'_2(y; g, g) = \bar{q}_2(Y - y; g, g). \quad (44)$$

This means that under the duality transformation (36) each solution is transformed into itself (solution 1) or into another solution (solutions 2 and 2'), and the full set of solutions $\{\bar{p}, \bar{q}\}$ is invariant under the duality transformation of $p \leftrightarrow q$ and $y \rightarrow Y - y$.

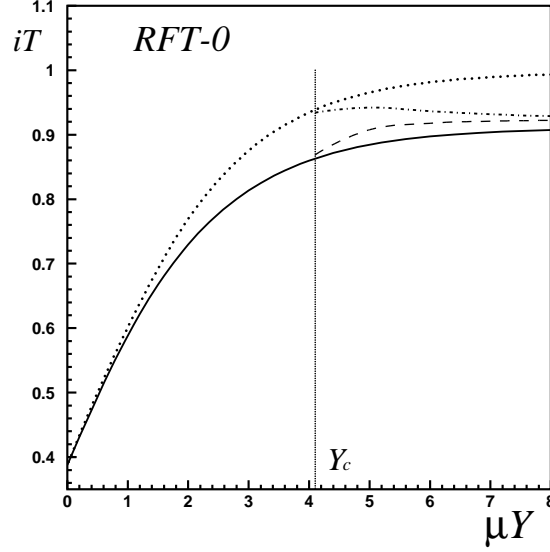


Figure 4: *Scattering amplitude $iT = 1 - S$ from RFT-0 for $g_1 = g_2 = 0.7$ at $\mu/\lambda = 5$ as a function of rescaled rapidity μY in various approximations: dotted line represents amplitude obtained from the symmetric solution 1, dashed line correspond to the pair of asymmetric solutions $\{2, 2'\}$, the dash-dotted line accounts for sum of contributions from $\{1, 2, 2'\}$ and the solid line represents the full quantum solution of the problem. (the plot is taken from [46]).*

The observed phenomenon of spontaneous symmetry breaking occurs at the classical level. At the quantum level, however, the projectile-target symmetry should hold¹. One sees it, for instance, from the form of the S -matrix in the semi-classical approximation using the three solutions $\{1, 2, 2'\}$. The calculation of the quantum weights for $Y > Y_c$ was performed in [41] leading to,

$$S(Y; g_1, g_2) \simeq -\exp\{-\mathcal{A}_{RFT-0}[\bar{q}_1, \bar{p}_1; Y]\} + \exp\{-\mathcal{A}_{RFT-0}[\bar{q}_2, \bar{p}_2; Y]\} + \exp\{-\mathcal{A}_{RFT-0}[\bar{q}'_2, \bar{p}'_2; Y]\}, \quad (45)$$

where the minus sign of the first term comes from the complex phase factors picked up by the trajectory 1 at the turning points. One sees that the symmetry between the projectile and the target is restored for the S -matrix already at the semi-classical level, by summation over the complete set of (asymmetric and symmetric) classical trajectories. It is interesting to ask, however, whether there could be some signs of the symmetry breaking found at the classical level, that would be seen for more exclusive observables, like for the rapidity distribution of produced particles. In principle, such a *classical measurement* should destroy the quantum coherence and select just one of the classical solutions. If this were true, it should lead to an asymmetric particle production between the identical projectile and target in individual events.

¹Due to quantum coherence in finite quantum systems the spontaneous symmetry breaking does not happen. It is only possible in the thermodynamical limit when the coherence between the asymmetric configurations is broken.

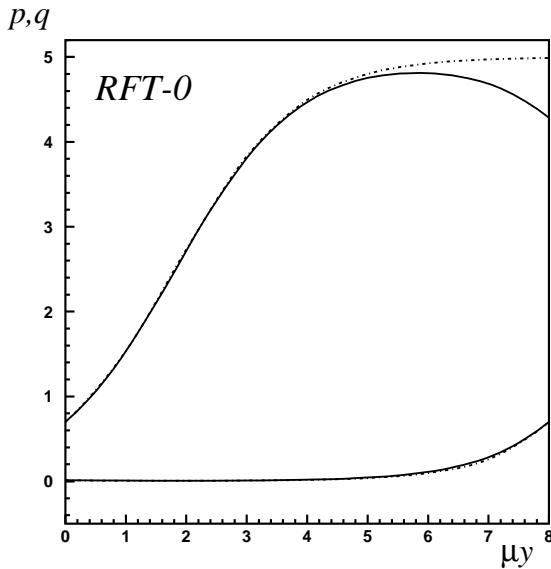


Fig. 5-a

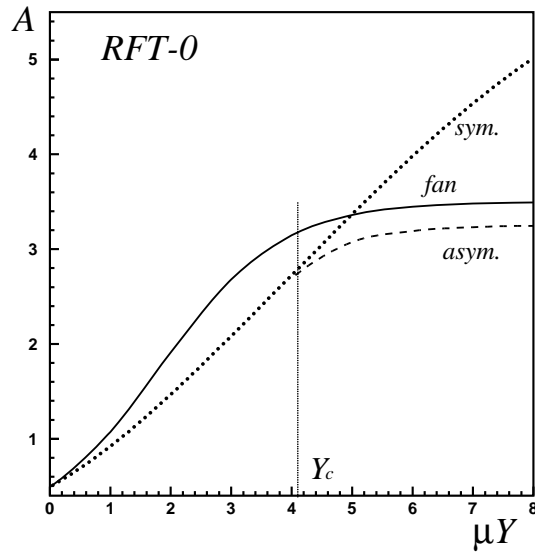


Fig. 5-b

Figure 5: Comparison of the classical asymmetric solution of the full theory to the solution of the equation resumming the fan diagrams: a) the trajectory: $\bar{q}_2(y)$ (upper solid line) and $\bar{p}_2(y)$ (lower solid line) and the trajectories of the fan equation $\bar{q}_f(y)$ and $\bar{p}_f(y)$ (upper and lower dotted lines respectively) for the total rapidity $\mu Y = 8$ as a function of μy ; b) the action for the classical solutions: the asymmetric one (the dashed line) the symmetric one (the dotted line) versus the action resumming pomeron fan diagrams as a function of μY .

It is instructive to compare various approximations to the scattering amplitude $iT = 1 - S$. Thus, we plot in Fig. 4a the scattering amplitude evaluated in the semi-classical approximation assuming that it is dominated by the symmetric solution 1 (which should be valid for $Y < Y_c$), by the pair of asymmetric solutions $\{2, 2'\}$, (which should hold for $Y \gg Y_c$), and including contributions to the S -matrix of all three solutions for $Y > Y_c$. We expect the last and the most complete choice be the most accurate. The comparison to the exact quantum evaluation of the scattering amplitude² (the continuous curve) to the various semi-classical evaluations reveals, however, that the contribution of $\{2, 2'\}$ approximates the exact answer best. It may be a coincidence or a hint on the subtle point of how to treat contributions to the S -matrix from subleading trajectories. We leave the issue for further studies.

3.3 Fan dominance

Anticipating the results of the next section, let us briefly mention an interesting feature of asymmetric solutions for Y being significantly larger than the critical rapidity Y_c and for sources $g_1, g_2 \ll \mu/\lambda$. Then, one of the fields, say q , grows with the increasing rapidity. The other field, p , assumed to take the value of $g_2 \ll \mu/\lambda$ at rapidity Y decreases further for decreasing y . Therefore the term involving p^2 in Lagrangian

²The curve was obtained in the course of our ongoing study of the RFT-0 [46], where we solve the RFT-0 both at the classical and the quantum level. We leave the description of the details to that paper.

(34) is of little importance and it may be neglected. Thus, one ends up with the evolution equations of the system with the absent vertex for the pomeron splitting. This evolution equation resums the *fan diagrams* of the merging fields q , and it will be referred to as the *fan equation*.

We exemplify in Fig. 5a the similarity of the asymmetric solution of the full theory $\{\bar{q}_2(y), \bar{p}_2(y)\}$ to the solution of the equation resumming the fan diagrams $\{\bar{q}_f(y), \bar{p}_f(y)\}$. The figure was obtained with $\mu/\lambda = 5$, $g_1 = g_2 = 0.7$, and we set $\mu Y = 8 \simeq 2\mu Y_c$. The smaller fields $p_2(y)$ and $p_f(y)$ turned out to overlap with high accuracy. We find some noticeable difference between $q_2(y)$ and $q_f(y)$ only at higher values of μy . We checked that the asymmetric solution is closer to the “fan equation” solution if Y is larger and g_1 and g_2 are smaller. The results of evaluation of the action corresponding to $\{\bar{q}_2(y), \bar{p}_2(y)\}$, $\{\bar{q}_f(y), \bar{p}_f(y)\}$ and to the symmetric classical solution $\{\bar{q}_1(y), \bar{p}_1(y)\}$ are shown in Fig. 5b. Again, the solution to the fan equation yields the action that reasonably well approximates the action $\mathcal{A}_{RFT-0}(\bar{q}_2(y; g, g), \bar{p}_2(y; g, g); Y)$ of the dominant trajectory.

We find this convergence of the classical system to the fan-dominated regime to be a rather surprising effect especially in view of the fact that we started from completely symmetric boundary conditions. A similar observation, however, was made in slightly different realisation of RFT-0, with a non-zero four pomeron coupling [45]. It will be very interesting to check whether a similar phenomenon occurs for the theory of interacting QCD pomerons.

4 Solutions of the Braun equations

4.1 Parameters and the solving procedure

Classical equations of motion (27) and (28) for the effective pomeron fields $f(y, k^2)$ and $f^\dagger(y, k^2)$ were solved numerically for various values of the total rapidity Y of the scattering. We chose a fixed coupling constant $\alpha_s = 0.2$. The boundary conditions were assumed to be symmetric

$$f_A(k^2) = f_B^\dagger(k^2) = \frac{N}{\pi R^2} \frac{k^4}{Q_0^4 + k^4}. \quad (46)$$

The form of the input condition was inspired by the properties of a saturated gluon distribution in the nucleon. Thus we set $R^2 = 8 \text{ GeV}^{-2}$ in order to match the preferred value of the nucleon size. The scale $Q_0^2 = 0.5 \text{ GeV}^2$ corresponds to the saturation scale for $10^{-3} < x < 10^{-2}$. The overall normalisation factor $N = 2$ so that the collinear gluon distribution obtained from the input is similar to the actual collinear gluon distribution $xg(x, Q^2)$ in the proton for $10^{-3} < x < 10^{-2}$ and for moderate Q^2 . Let us stress that we made that choice only to pin down the physically relevant ranges of parameters.

The numerical solution was based on a Chebyshev interpolation method in the variable $\log(k^2)$ used to discretize the differentio-integral equations (27) and (28). In order to solve the two-point boundary problem, we applied the iterative procedure defined by Braun [35]. Thus, in each iteration the evolution in rapidity of one of the field $f(y, k^2)$ or $f^\dagger(y, k^2)$ was performed while the other field was set to its value obtained in the previous iteration. In the odd iterations, the field $f(y, k^2)$ was evolved from its initial value $f_A(k^2)$ from $y = 0$

to $y = Y$ and the field $f^\dagger(y, k^2)$ was kept fixed (in the first iteration $f^\dagger(y, k^2)$ was set identically to zero). In the even iterations $f^\dagger(y, k^2)$ was evolved from $y = Y$ down to $y = 0$ with the initial value $f_B^\dagger(k^2)$ at $y = Y$. The iterations were continued until a fixed point of $f(y, k^2)$ and $f^\dagger(y, k^2)$ was reached. Clearly, at the fixed point of the iterative procedure the fields $\{f(y, k^2), f^\dagger(y, k^2)\}$ solve the system of Braun equations (27) and (28) with boundary conditions (29). The method was found to be stable and robust and no problems with convergence occurred of the kind reported in [35]. A disadvantage of the iterative method is that it may be only used to find the solutions which represent the attractive fixed points of the procedure. Unfortunately, we expect from the analysis of solutions of the RFT in zero transverse dimensions, that the solution to Braun equations is not unique at larger rapidities and there should exist multiple solutions. Therefore it is probable that the iterative method finds only some of them. On the other hand, one hopes that the most relevant solutions that minimize the action may become an attractive fixed points of a reasonable iterative procedure. Some more arguments in favour of this scenario will be given based on the properties of the found solutions.

4.2 Properties of solutions and spontaneous symmetry breaking

In what follows we shall describe the properties of the solutions to the Braun equations for rapidities of the scattering $Y = 6, 8, 10, 12$ and $Y = 16$. The pomeron field $f^\dagger(y, k^2)$ will be often presented as a function of the transformed rapidity $y' = Y - y$, so that the initial condition for f^\dagger is imposed at $y' = 0$. In the figures we shall plot $f(y, k^2)/k^2$ and $f^\dagger(y', k^2)/k^2$ unless we explicitly specify differently. Such a choice of variables is preferred by their *solitonic* behaviour in the case of the BK equation. For future reference, let us introduce the notation $f^{\text{BK}}(y, k^2)$ to represent the solution to the BK equation with the input given by (46). In the figures the label “Input” is used for $f_A(k^2)/k^2$, where $f_A(k^2)$ defined by (46).

In Fig. 6a and Fig. 6b we show the solutions to the Braun equations for $Y = 6$ and $Y = 8$ respectively. Solid lines denote $f(y, k^2)/k^2$ and $f^\dagger(y', k^2)/k^2$ is shown with points. The curves are plotted for y varying from zero to Y in the steps of one. Clearly, in both cases the solutions are symmetric, $f(y, k^2) = f^\dagger(Y - y, k^2)$. Anticipating Fig. 12a, we point out that the solutions exhibit a similar behaviour to solutions of the BK equation at large gluon momenta k^2 . At small momenta, below the saturation scale of the BK equation, $f(y, k^2)$ and $f^\dagger(y', k^2)$ are much flatter than $f^{\text{BK}}(y, k^2)$.

We find that the symmetry between f and f^\dagger breaks down at some critical rapidity $Y_c \simeq 9$. For $Y > Y_c$ only the asymmetric solutions are found, for which $f(y, k^2) \neq f^\dagger(Y - y, k^2)$, compare Fig. 7a (Fig. 7b) and Fig. 8 (Fig. 9) for $Y = 10$ ($Y = 16$). Thus, the symmetry between the projectile and the target is spontaneously broken for individual classical solutions, in close analogy with the phenomenon appearing in RFT-0, described in detail in Sec. 3.2. The asymmetry between $f(y, k^2)$ and $f^\dagger(Y - y, k^2)$ vanishes at $Y = Y_c$, so the asymmetric solutions connect smoothly to the symmetric one at $Y = Y_c$ and the asymmetry builds up gradually with increasing Y . Certainly, the numeric value of the critical rapidity Y_c is not universal, it depends on the boundary conditions and on the value of α_s . It is important to note, that for each asymmetric solution $\{f, f^\dagger\}$ there exists a complementary solution $\{f', f'^\dagger\}$, such that $f'(y, k^2) = f^\dagger(Y - y, k^2)$ and $f'^\dagger(Y - y, k^2) = f(y, k^2)$, reflecting the symmetry between the projectile and the target encoded in the

action and the symmetric boundary conditions. Knowing that, in the further analysis of the solutions we choose arbitrarily that $f(y, k^2)$ is the larger field and $f^\dagger(y', k^2)$ is the smaller one.

For $Y > Y_c$, the general features of the larger field f are the following. At $Y \simeq Y_c$ the solution is similar to the symmetric solutions found for $Y < Y_c$. With increasing Y a pattern appears of a traveling wave, that is formation of a peak of $f(y, k^2)/k^2$ traveling towards larger values of $\log(k^2)$ with increasing rapidity with only small changes of the shape, see Fig. 7a and Fig. 7b. Recall, that it is behaviour characteristic for the BK equation [29]. The similarity of the solution to the BK solution will be investigated in more detail in Sec. 4.3.

The smaller field $f^\dagger(y, k^2)$ evolves differently, see Fig. 8 and Fig. 9. At $Y = Y_c$ it matches $f(Y - y, k^2)$ and for the increasing Y it experiences a significant overall suppression, stronger at larger Y . For instance, for $y \simeq Y/2$ the maximal value of $f^\dagger(y, k^2)/k^2$ is about an order of magnitude smaller than the maximal value of $f(y, k^2)/k^2$ at $Y = 10$ (compare Fig. 7a and Fig. 8) and about three orders of magnitude smaller at $Y = 16$ (see Fig. 7b and Fig. 9). Thus, we conjecture that in the limiting case of very large total rapidity Y , f^\dagger may be arbitrarily small except of the rapidities $y \simeq Y$ where the source term for f^\dagger is still important. In this context, it is instructive to study the y -dependence of $f^\dagger(y, k^2)/k^2$ at fixed k and compare it to $f(y, k^2)/k^2$. This comparison may be performed using Fig. 10. It turns out, that there appear two distinct regimes of evolution of $f^\dagger(y, k^2)/k^2$ with rapidity (at fixed momentum). Thus, if the field $f(y, k^2)/k^2$ is strong, the smaller field $f^\dagger(y', k^2)/k^2$ is exponentially suppressed with increasing y' , $f^\dagger(y', k^2)/k^2 \sim \exp(-\beta_1 y')$ with $\beta_1 \sim 1$, crudely. This is the region where the absorption of f^\dagger by f drives the evolution of f^\dagger . Then, when y is sufficiently small and the field $f(y, k^2)/k^2$ is weaker, the absorption becomes less relevant and $f^\dagger(y', k^2)/k^2$ grows exponentially with increasing y' , $f^\dagger(y', k^2)/k^2 \sim \exp(\beta_2 y')$ with the exponent $\beta_2 \simeq 0.4$ (with our choice of parameters) a value somewhat smaller than the BFKL intercept $\omega_0 = 4\bar{\alpha}_s \log(2) \simeq 0.53$. Note, that the characteristic rapidity y , at which the transition occurs from the strong absorption regime to the BFKL driven growth regime, depends on k . This is natural, as the field $f(y, k^2)/k^2$ becomes strong at larger values of y for larger k .

The shape of $f^\dagger(y', k^2)/k^2$ in k^2 exhibits some interesting features too, see Fig. 8 and Fig. 9. At small values of k , $f^\dagger(y', k^2)/k^2$ tends to a flat function. This should be compared with the case of the BK where $f^{\text{BK}}(y, k^2)/k^2 \sim k^2$ at small k . On the other hand, at large k^2 the decrease of $f^\dagger(y', k^2)/k^2$ with increasing k^2 is slower than the decrease of $f^{\text{BK}}(y, k^2)/k^2$. Thus, the overall picture is that $f^\dagger(y', k^2)/k^2$ is much flatter than $f^{\text{BK}}(y, k^2)/k^2$. As rather surprising comes an observation that effects of non-linear interactions in $f^\dagger(y', k^2)/k^2$ extend to very large values of momenta, causing a strong suppression of $f^\dagger(y', k^2)/k^2$ for all momenta up to $k = 10^3$ GeV, the value larger than the saturation scale generated by the large field $f(y, k^2)$, see for example Fig. 9. In fact, we checked that the suppression of $f^\dagger(y', k^2)/k^2$ in comparison to $f^{\text{BK}}(y, k^2)/k^2$ is strong even at $k = 10^5$ GeV (not shown).

The explanation of this phenomenon is the following. At large values of k^2 the input function $f_B^\dagger(k^2)$ was assumed to tend to a constant, in other words the anomalous dimension vanished for the input. For the BFKL or the BK system the rapidity evolution generates an anomalous dimension of $\gamma_0 \simeq 0.3 - 0.5$, strongly enhancing $f(y, k^2)$ for large k^2 and y . For $f^\dagger(y', k^2)$, however, the evolution and BFKL diffusion are almost completely blocked by large absorptive corrections coming from the interaction of $f^\dagger(y', k^2)$ with the large

field $f(y, k^2)$. Recall, that the input for $f^\dagger(y', k^2)$ resides in $y = Y$, where the value of the field $f(y, k^2)$ is the largest and so is the related saturation scale. Therefore, before any BFKL diffusion or enhancement of $f^\dagger(y', k^2)$ becomes possible (that is at sufficiently small y') strong suppression of $f^\dagger(y', k^2)$ occurs and the population of the large momenta region is initiated from a drastically reduced $f^\dagger(y', k^2)$.

In order to provide a more synthetic picture of the behaviour of $f(y, k^2)$ and $f^\dagger(y, k^2)$ we illustrate the case of $Y = 16$ with three dimensional plots of the solutions shown in Fig. 11. Note, that we plot in this figure $f^\dagger(y, k^2)$ instead of $f^\dagger(y', k^2)$. Thus, the input for f appears at $y = 0$ in Fig. 11a and the input of f^\dagger is plotted for $y = 16$ in Fig. 11b.

4.3 BK fan dominance

We have already related briefly the larger component $f(y, k^2)$ of the solution to the Braun equation to the solution of the Balitsky-Kovchegov equation $f^{\text{BK}}(y, k^2)$. A more detailed comparison is performed for $f(y, k^2)$ in Fig. 12 for $Y = 8$ and $Y = 12$, and in Fig. 14a for $Y = 16$. For $Y = 8$ where the solution is still symmetric, the difference between $f(y, k^2)$ (lines) and $f^{\text{BK}}(y, k^2)$ (points) is quite large and low k^2 and visible at large k^2 , see Fig. 12a. The difference is significantly reduced at $Y = 12$, as clearly seen in Fig. 12b. Here, $f(y, k^2)$ and $f^{\text{BK}}(y, k^2)$ almost exactly coincide except of some deviations for very small $k < 0.1$ GeV and $y > Y/2$. The overlap between $f(y, k^2)$ and $f^{\text{BK}}(y, k^2)$ is further improved at $Y = 16$. Evolution of the smaller component $f^{\dagger\text{BK}}(y', k^2)$ in the BK limit may be also performed by solving the system (27) and (28) with the terms neglected that were generated by the triple pomeron vertex corresponding to the pomeron splitting (the contribution to the action of \mathcal{L}_3^\dagger). The comparison of $f^\dagger(y', k^2)$ and $f^{\dagger\text{BK}}(y', k^2)$ is given for $Y = 8$, $Y = 12$ in Fig. 13 and for $Y = 16$ in Fig. 14b. In this case, the two different kinds of solutions coincide even better than the large components $f(y, k^2)$ and $f^{\text{BK}}(y, k^2)$.

Recall, that we also observed the similarity between the asymmetrical classical solutions of RFT-0 and the solution to the “fan equation”, the counterpart of the BK equation in zero transverse dimensions. Thus, the “fan dominance” at $Y \gg Y_c$ seems to be a generic feature of the interacting pomeron system. Even more can be said – the dependence of the QCD pomeron fields on the momentum might even enhance the convergence to the fan dominated system, compare Fig. 5 and Fig. 14. It happens probably because the deviations from the fan behavior appear at rapidities $y \rightarrow Y$, close to the source of the smaller field (which we chose to be $f^\dagger(y, k^2)$ for QCD pomerons and $p(y)$ for RFT-0) where the smaller field is not yet strongly suppressed by the evolution. In QCD, however, the input is localized at rather small values of gluon momenta k , whereas the larger field, $f(y, k^2)$, is concentrated around the saturation scale $Q_s(y)$ which is large for $y \rightarrow Y$. Therefore, the relatively large $f^\dagger(y', k^2)$ in this rapidity domain affects only the tail of low momenta in $f(y, k^2)$, with little relevance for the dynamics of the system. Possible implications of the “fan dominance” are discussed in the Sec. 5.

As the last point, let us comment shortly on the issue of multiple solutions to the Braun equations out of which only some can be found by the iterative solving procedure. Recall, that in the semi-classical approximation of the system moving in the Euclidean time, the most relevant are the trajectories with the lowest value of the action. We have no proof that the asymmetric classical trajectories that were found

in this paper fulfill this requirement. Numerous similarities of the patterns of solutions obtained in the interacting QCD Pomeron Field Theory and RFT-0 are, fortunately, reassuring. In both cases there exists a symmetric solution at low rapidity and two asymmetric solutions at $Y > Y_c$. In both theories the “fan dominance” phenomenon was found. Therefore, one may conjecture that the asymmetric solutions of the Braun equations, indeed, are the classical trajectories with the lowest action, in analogy to the explicit result obtained in RFT-0.

4.4 Summary of the results

Let us summarize the presentation of results with a recapitulation of the most important observations:

1. Solutions $\{f, f^\dagger\}$ of the Braun equations with symmetric boundary conditions split into two different types: the symmetric solution $f(y, k^2) = f^\dagger(Y - y, k^2)$ that dominates below the critical rapidity Y_c and a pair of the asymmetric solutions, found for $Y > Y_c$.
2. The asymmetric solutions exhibit the feature of “fan dominance” which becomes more accurate with increasing Y . Due to the smallness of one of the field the system evolves as if one of the triple pomeron vertices (describing splitting or merging) was absent. The larger field is close to the solution of the BK equation.
3. Unitarity corrections for the smaller field $f^\dagger(y', k^2)$ are very pronounced at $Y \gg Y_c$ leading to very strong damping (even 2-3 orders of magnitude at $Y = 16$, and increasing with Y) of the smaller field and flattening of the shape of $f^\dagger(y', k^2)/k^2$. We find that $f^\dagger(y', k^2) \sim k^2$ for $k^2 < Q_s^2(y)$, where $Q_s(y)$ is the saturation scale generated by the larger field $f(y, k^2)$.
4. The symmetric solution below the critical rapidity is significantly flatter at low momenta than the BK solution. At large momenta the decrease of the symmetric solution is power-like, with an exponent close to that of BK, but the solution to the Braun system is somewhat smaller than the BK solution from the same input.

5 Discussion

The breaking of the projectile-target symmetry which we have found above the critical rapidity is rather surprising and it calls for an explanation and interpretation. To our understanding the mechanism of this breaking is the following. Suppose that we have a symmetric situation in the system of the two evolving pomeron fields $\{f, f^\dagger\}$. If the fields are small and therefore weakly interacting then the interaction is only a small perturbation and the symmetry of the action and of the initial conditions should be reflected in the solution. This is, indeed, the case for the Braun equations with the total rapidity Y smaller than the critical value Y_c . Let us consider now a symmetric system of pomeron fields when the fields are already strong due to their rapidity evolution. Then, the fields absorb intensively each other. The combination of the multiplication of the fields and the strong mutual absorption is a potential source of instability. Namely,

if we perturb the symmetric system of fields in this regime by, say, small increase of the value of the field f then the absorption of f^\dagger by interaction with f will be also increased. Thus, after this perturbation f^\dagger should become smaller. This results, however, in a smaller absorption of the field f , leading to yet higher values of f , so that the instability will self-amplify generating finally an asymmetric configuration. Of course, whether this scenario is realized, depends on the particular form of the action. From our numerical results we conclude that this is, indeed, the case for the interacting pomeron fields above the critical rapidity in the classical approximation. It is curious that in the earlier study of the Braun equations the symmetry breaking was not found [35]. Instead, there was reported an instability of the iterative procedure at critical values of rapidity, depending on the input. It was interpreted as a possible indication of a phase transition. We speculate that those instabilities might be, in fact, signs of emergence of asymmetrical solutions.

The key question arises what happens with the spontaneous symmetry breaking (SSB) when the quantum effects are considered. Strictly speaking, for finite systems SSB does not occur at the quantum level. The ground state of the finite system in which the symmetry is spontaneously broken at the classical level is a symmetric coherent superposition of non-symmetric states. It is only in the thermodynamic limit when the SSB may take place in a quantum system. In the case of the reggeon field theory situation is even more complicated due to the fact that the evolution variable (the rapidity) would correspond to imaginary time in the Schrödinger picture. The consequences of the fact were investigated in detail in the framework of the reggeon field theory with impact parameter dependence (RFT-b) [47]. It turns out that in RFT-b the degenerate vacua communicate by quantum evolution irrespectively to the extension of the system in the transverse space and the symmetry of quantum theory is maintained even in the thermodynamical limit. The communication was found to be realized by solitons in the impact parameter plane smoothly interpolating between the two asymmetric vacua. In addition, the bifurcation of the classical solution at $Y = Y_c$ would indicate presence of a singularity of the S -matrix³ in Y . This singularity is not expected to be present in the complete quantum theory.

It should be stressed, however, that in this paper we do not address the issue of properties of the QCD pomeron field theory in the thermodynamical context. The goal is rather to get insight into scattering of two strong sources of colour field e.g. the nuclei. In collisions of two nuclei the measurements give access not only to the total cross sections but also to extended information about the kinematics of the produced particles on the event-by-event basis. This is a classical measurement which, necessarily, breaks the quantum coherence. Therefore it is possible that such measurement selects one of the classical pomeron field trajectories which exhibit the symmetry breaking between the target and the projectile. In fact, the rapidity dependence of the saturation scale is different for the two asymmetric solutions of the Braun equations: for one of the solutions the saturation scale increases from the target to the projectile, while for the other it decreases. The average transverse momentum \bar{p}_T of the emitted particles should be correlated with the saturation scale. Hence, a classical measurement of the event should select one of the asymmetric solutions and it could exhibit some asymmetry in rapidity distribution of the produced particles. The pattern may be somewhat obscured, however, when the dependence on the transverse position is taken into account. In the collision the regions separated in the impact parameter are only weakly correlated and, in principle, it is possible that different

³We thank Lev Lipatov for this point.

domains in the transverse space are dominated by different asymmetric solutions of Braun equations. This would make the possible effects of asymmetry more subtle and harder to disentangle.

One of the question which should be addressed is what observables could serve as experimental signatures of the asymmetry between the target and the projectile in heavy ion collisions. Certainly, the total cross section carries no information about the details of the evolution, so one should focus on more detailed observables. As a first guess we would propose investigation of the average transverse momentum $\bar{p}_T = \sqrt{\langle p_T^2 \rangle}$ of the particles produced in central collisions of heavy ions as a function of rapidity y in the c.m.s. frame on the event-by-event basis. With the symmetry between the target and the projectile being preserved the observable $\bar{p}_T(y)$ measured for individual events should be the same after changing the definition of rapidity $y \rightarrow -y$. If the symmetry is broken in the event, however, $\bar{p}_T(y)$ should exhibit a clear trend.

At this stage, we are not able to determine whether the symmetry breaking is a real physical phenomenon or an artifact of the effective theory of interacting pomerons. Needless to say, the framework of Braun equations relies on several assumptions that are far from being proven. First of all, it is not clear if the pomerons are valid degrees of freedom in dense and strongly interacting gluonic systems. One may argue that at high density the pomerons overlap and melt down to gluons, whose dynamics may be significantly different from the dynamics of the pomeron fields. Secondly, in the present analysis we neglected quantum effects related to the pomeron loops. The impact of the quantum effects on the phenomenon of symmetry breaking is unknown. Moreover, we neglected contribution of vertices with more than three pomerons. In addition, the NLL corrections to the BFKL pomeron kernels and to the triple pomeron vertices are neglected in the present form of Braun equations. This causes the BFKL intercept to be roughly two times too large. This means that the spontaneous breaking of the projectile-target symmetry should occur (if it occurs) at much higher rapidities than it may be deduced from the analysis employing the LL BFKL kernel, perhaps for energies beyond reach of the LHC. On the other hand, the value of $\alpha_s = 0.2$ underestimates significantly the expected value of α_s for the triple pomeron vertex (recall that the vertex is proportional to α_s^2) and with a more realistic value a smaller Y_c would be predicted. Finally, in order to evaluate relevance of the effect the input conditions should be carefully tuned to embody the available information on the unintegrated gluon density in the nuclei, including the impact parameter profiles. Keeping in mind all these reservation, we believe that further theoretical and experimental studies of the issue should be carried out.

Leaving the issue of the symmetry breaking, we point out that the “fan dominance” phenomenon at $Y > Y_c$ found in the case of the symmetric boundary conditions should be even more pronounced when the projectile and the target are different. This might provide some basis for the use of the BK equation to describe the saturation effects in the DIS at low Q^2 . Strictly speaking, the BK equation is valid for a small perturbative probe scattering off a large target, for instance a nucleus. This condition is, certainly, not fulfilled for almost real photon scattering off a proton, nor it is for the diffractive DIS, dominated by scattering of large dipoles. Still, the fits based on the BK amplitudes are very successful in both cases. The “fan dominance” in the symmetric Braun system could provide some support for those applications of the BK equation, although it is fair to admit that the use of Braun equations to processes of this kind is not on the firm ground either.

The Braun equations are a minimal extension of the very fruitful concept of the BK equation, that embodies the symmetry between the pomeron fields f and f^\dagger at the level of the action. Possibly, this extension may also find some interesting phenomenological applications. Following Braun we state that description of heavy ion collisions is the obvious application of the equations. In that case the quantum loops should have only a subleading effect and the approximate treatment of the dependence transverse position is certainly sufficient. A more challenging is an application of the formalism to the vital problem of understanding of pp collisions at the LHC energies. In particular, we have in mind the description of underlying event, particle production (see e.g. [48, 49]), diffractive processes and determination of the gap survival factor in hard exclusive processes, like for instance the exclusive Higgs boson production. Expanding on this example, the exclusive Higgs boson production is an important process which is probable to be measured at the LHC [50]. It was shown, that the theoretical understanding of the cross section for this process requires a good control of the hard rescattering corrections [51]. The framework of the semi-classical field theory of the interacting pomerons may serve as a tool to perform the necessary resummations of multi-pomeron diagrams and to obtain improved estimates of the gap survival factor. All the listed applications are, however, non-trivial as they require inclusion of NLL BFKL corrections and, possibly, more accurate treatment of the dynamics of the system in the transverse position space.

In the last part of this section we will briefly mention some intriguing open questions. Thus, it would be interesting to investigate the stochastic QCD evolution of the color glass condensate using the realization of the semi-classical approximations in which only the tree topologies of the pomeron are retained. In analogy to the Pomeron Field Theory, this limit should be simpler than the accurate treatment also in the CGC formulation. Furthermore, a similar analysis of the Pomeron Field Theory should be possible after inclusion of the pomeron vertices at which more than three pomeron fields. The form of those vertices may be predicted using the conjectured conformal symmetry of the pomeron field theory [52]. While the conformal symmetry of the effective field theory of the interacting pomerons in the EGLLA was not explored in the present study, it constitutes, certainly, a key ingredient of the structure of the complete theory. Thus, it is mandatory to account for it in similar future studies.

Finally, let us refer to recent developments on the connection between the superconformal gauge theories in four dimensions and the superstring theory on the $AdS_5 \times S^5$ background [1]. Using the AdS/CFT duality it was found that the BFKL pomeron in gauge theories corresponds to the graviton Regge trajectory in the AdS space [53]. Thus, it is desirable to find an interpretation of the effective pomeron field theory at the string side, perhaps in terms of gravity. Curiously enough, it was discovered recently that collisions of heavy ions possess a dual gravitational description [54]. The dual of the scattering is given by a collision of two gravitational shock waves in which black holes can be formed. Example of such a black hole solution being produced, that moves in the fifth dimension of the Anti de Sitter space was found [55]. Thus, the relation between the fifth dimension in the AdS and the gluon virtuality inspires a question about the possible connection of the black hole to the BK traveling wave solution, whose existence we established in the classical pomeron field theory. Therefore, it is important to verify whether phenomena analogous to the symmetry breaking between the target and the projectile and the “fan dominance” also happen in the string world.

6 Conclusions

Effective field theory of interacting QCD pomerons was investigated in the semi-classical limit, as a framework to describe high energy scattering of two nuclei. The effective action was proposed in the form using the pomeron amplitudes, as the basic degrees of freedom, related to the unintegrated gluon densities in the linear regime. Triple pomeron vertices in the momentum space accounted for the pomeron merging and splitting. Arbitrariness in the choice of the direction of evolution in rapidity required both the vertices to be identical and induced the self-duality of the action. This symmetry combined with symmetric initial conditions defined the scattering problem to be symmetric under the interchange of the target and the projectile. Classical pomeron field equations (*Braun equations*) were re-derived and solved numerically. The solutions were found that were invariant under the projectile-target symmetry only for scattering rapidities Y smaller than a critical (non-universal) value Y_c . For $Y > Y_c$ the projectile-target symmetry turned out to be *spontaneously broken*. Above the critical rapidity, the solutions converged to the solutions of the Balitsky-Kovchegov equation, the phenomenon which we called the *BK fan dominance*. A very similar pattern of symmetry breaking and the fan dominance occurs also in the Reggeon Field Theory in zero transverse dimensions, which suggests that this is a generic feature of the interacting pomeron system. We discussed possible consequences of those observations for the phenomenology of heavy ion collisions and the physics of pp scattering at the LHC. Finally, we suggested that the results of this paper may have counterparts in the dual description of heavy ion collisions in terms of scattering of two gravitational shock waves in the Anti de Sitter space in five dimensions.

Acknowledgments

We are especially grateful to Jochen Bartels for his continued interest in this work and numerous enlightening discussions. We thank Mikhail Braun, Krzysztof Golec-Biernat, Eugene Levin, Lev Lipatov and Alfred Mueller for discussions and useful comments. S.B. thanks the Minerva foundation for its support and L.M. gratefully acknowledges the support of the grant of the Polish State Committee for Scientific Research No. 1 P03B 028 28.

References

- [1] J. M. Maldacena, Adv. Theor. Math. Phys. **2** (1998) 231 [Int. J. Theor. Phys. **38** (1999) 1113]; E. Witten, Adv. Theor. Math. Phys. **2** (1998) 253; O. Aharony, S. S. Gubser, J. M. Maldacena, H. Ooguri and Y. Oz, Phys. Rept. **323** (2000) 183.
- [2] L. N. Lipatov, Sov. J. Nucl. Phys. **23** (1976) 338 [Yad. Fiz. **23** (1976) 642]; E. A. Kuraev, L. N. Lipatov and V. S. Fadin, Sov. Phys. JETP **45** (1977) 199 [Zh. Eksp. Teor. Fiz. **72** (1977) 377]; I. I. Balitsky and L. N. Lipatov, Sov. J. Nucl. Phys. **28** (1978) 822 [Yad. Fiz. **28** (1978) 1597].
- [3] L. N. Lipatov, Phys. Rept. **286** (1997) 131.

- [4] V. S. Fadin and L. N. Lipatov, Phys. Lett. B **429** (1998) 127; M. Ciafaloni and G. Camici, Phys. Lett. B **430** (1998) 349; V. S. Fadin and R. Fiore, Phys. Lett. B **610** (2005) 61 [Erratum-ibid. B **621** (2005) 61]; V. S. Fadin and R. Fiore, Phys. Rev. D **72** (2005) 014018.
- [5] I. Balitsky, Nucl. Phys. B **463** (1996) 99.
- [6] J. Jalilian-Marian, A. Kovner and H. Weigert, Phys. Rev. D **59** (1999) 014015; J. Jalilian-Marian, A. Kovner, A. Leonidov and H. Weigert, Phys. Rev. D **59** (1999) 014014; E. Iancu, A. Leonidov and L. D. McLerran, Nucl. Phys. A **692** (2001) 583; E. Iancu, A. Leonidov and L. D. McLerran, Phys. Lett. B **510** (2001) 133; E. Iancu and L. D. McLerran, Phys. Lett. B **510** (2001) 145; E. Ferreiro, E. Iancu, A. Leonidov and L. McLerran, Nucl. Phys. A **703** (2002) 489.
- [7] A. H. Mueller, Nucl. Phys. B **415** (1994) 373.
- [8] E. Iancu, A. H. Mueller and S. Munier, Phys. Lett. B **606** (2005) 342; E. Iancu and D. N. Triantafyllopoulos, Nucl. Phys. A **756** (2005) 419; A. H. Mueller, A. I. Shoshi and S. M. H. Wong, Nucl. Phys. B **715** (2005) 440; S. Munier, Nucl. Phys. A **755** (2005) 622; E. Levin and M. Lublinsky, Nucl. Phys. A **763** (2005) 172; E. Iancu and D. N. Triantafyllopoulos, Phys. Lett. B **610** (2005) 253; R. Enberg, K. Golec-Biernat and S. Munier, Phys. Rev. D **72** (2005) 074021; D. N. Triantafyllopoulos, Acta Phys. Polon. B **36** (2005) 3593.
- [9] J. Bartels, Z. Phys. C **60** (1993) 471.
- [10] J. Bartels and M. Wüsthoff, Z. Phys. C **66** (1995) 157.
- [11] J. Bartels and C. Ewerz, JHEP **9909** (1999) 026.
- [12] C. Ewerz, Phys. Lett. B **512** (2001) 239.
- [13] C. Ewerz and V. Schatz, Nucl. Phys. A **736** (2004) 371.
- [14] T. Bittig and C. Ewerz, Nucl. Phys. A **755** (2005) 616.
- [15] Y. V. Kovchegov, Phys. Rev. D **60** (1999) 034008.
- [16] Y. V. Kovchegov, Phys. Rev. D **61** (2000) 074018.
- [17] K. Golec-Biernat and M. Wüsthoff, Phys. Rev. D **59** (1999) 014017.
- [18] K. Golec-Biernat and M. Wüsthoff, Phys. Rev. D **60** (1999) 114023.
- [19] E. Levin and K. Tuchin, Nucl. Phys. B **573** (2000) 833; M. Braun, Eur. Phys. J. C **16** (2000) 337; H. Weigert, Nucl. Phys. A **703** (2002) 823; M. Lublinsky, E. Gotsman, E. Levin and U. Maor, Nucl. Phys. A **696** (2001) 851; N. Armesto and M. A. Braun, Eur. Phys. J. C **20** (2001) 517; K. Golec-Biernat, L. Motyka and A. M. Staśto, Phys. Rev. D **65** (2002) 074037; G. Chachamis, M. Lublinsky and A. Sabio Vera, Nucl. Phys. A **748** (2005) 649.
- [20] K. Golec-Biernat and A. M. Staśto, Nucl. Phys. B **668** (2003) 345.

- [21] K. Rummukainen and H. Weigert, Nucl. Phys. A **739** (2004) 183.
- [22] E. Levin and K. Tuchin, Nucl. Phys. A **691** (2001) 779; J. Kwieciński and A. M. Staśto, Phys. Rev. D **66** (2002) 014013; E. Iancu, K. Itakura and L. McLerran, Nucl. Phys. A **708** (2002) 327.
- [23] A. H. Mueller and D. N. Triantafyllopoulos, Nucl. Phys. B **640** (2002) 331; D. N. Triantafyllopoulos, Nucl. Phys. B **648** (2003) 293; L. Motyka, Phys. Lett. B, in print; arXiv:hep-ph/0509270.
- [24] E. Gotsman, E. Levin, M. Lublinsky and U. Maor, Eur. Phys. J. C **27** (2003) 411;
- [25] K. Kutak and J. Kwieciński, Eur. Phys. J. C **29** (2003) 521; K. Kutak and A. M. Staśto, Eur. Phys. J. C **41** (2005) 343.
- [26] E. Iancu, K. Itakura and S. Munier, Phys. Lett. B **590** (2004) 199.
- [27] A. M. Staśto, K. Golec-Biernat and J. Kwieciński, Phys. Rev. Lett. **86** (2001) 596.
- [28] J. Bartels and E. Levin, Nucl. Phys. B **387** (1992) 617.
- [29] S. Munier and R. Peschanski, Phys. Rev. Lett. **91** (2003) 232001; S. Munier and R. Peschanski, Phys. Rev. D **69**, 034008 (2004); S. Munier and R. Peschanski, Phys. Rev. D **70**, 077503 (2004).
- [30] J. Bartels, K. Golec-Biernat and H. Kowalski, Phys. Rev. D **66** (2002) 014001.
- [31] N. Timneanu, J. Kwieciński and L. Motyka, Eur. Phys. J. C **23** (2002) 513.
- [32] H. Kowalski and D. Teaney, Phys. Rev. D **68** (2003) 114005.
- [33] H. Kowalski, L. Motyka and G. Watt, in preparation; K. Kowalski, talk given at XIV International Workshop on Deep Inelastic Scattering, April 2006, Tsukuba, Japan.
- [34] M. A. Braun, Phys. Lett. B **483** (2000) 115.
- [35] M. A. Braun, Eur. Phys. J. C **33** (2004) 113.
- [36] M. A. Braun, Phys. Lett. B **632** (2006) 297.
- [37] A. H. Mueller and A. I. Shoshi, Nucl. Phys. B **692** (2004) 175.
- [38] I. Balitsky, Phys. Rev. D **70** (2004) 114030; I. Balitsky, Phys. Rev. D **72** (2005) 074027.
- [39] D. Amati, L. Caneschi and R. Jengo, Nucl. Phys. B **101** (1975) 397.
- [40] R. Jengo, Nucl. Phys. B **108** (1976) 447; D. Amati, M. Le Bellac, G. Marchesini and M. Ciafaloni, Nucl. Phys. B **112** (1976) 107; M. Ciafaloni, M. Le Bellac and G. C. Rossi, Nucl. Phys. B **130** (1977) 388.
- [41] M. Ciafaloni, Nucl. Phys. B **146** (1978) 427.

- [42] A. Kovner and M. Lublinsky, Phys. Rev. Lett. **94** (2005) 181603; J. P. Blaizot, E. Iancu, K. Itakura and D. N. Triantafyllopoulos, Phys. Lett. B **615** (2005) 221; Y. Hatta, E. Iancu, L. McLerran, A. Staśto and D. N. Triantafyllopoulos, Nucl. Phys. A **764** (2006) 423; C. Marquet, A. H. Mueller, A. I. Shoshi and S. M. H. Wong, Nucl. Phys. A **762** (2005) 252.
- [43] A. Kovner and U. A. Wiedemann, Phys. Rev. D **66** (2002) 051502; A. Kovner and U. A. Wiedemann, Phys. Lett. B **551** (2003) 311.
- [44] P. Rembiesa and A. M. Staśto, Nucl. Phys. B **725** (2005) 251; A. I. Shoshi and B. W. Xiao, Phys. Rev. D **73** (2006) 094014; A. I. Shoshi and B. W. Xiao, arXiv:hep-ph/0605282.
- [45] M. Kozlov and E. Levin, arXiv:hep-ph/0604039.
- [46] S. Bondarenko and L. Motyka, in preparation.
- [47] D. Amati, G. Marchesini, M. Ciafaloni and G. Parisi, Nucl. Phys. B **114** (1976) 483; V. Alessandrini, D. Amati and M. Ciafaloni, Nucl. Phys. B **130** (1977) 429.
- [48] F. Gelis, A. M. Staśto and R. Venugopalan, arXiv:hep-ph/0605087.
- [49] E. Iancu, C. Marquet and G. Soyez, arXiv:hep-ph/0605174.
- [50] V. A. Khoze, A. D. Martin and M. G. Ryskin, Eur. Phys. J. C **14** (2000) 525; A. De Roeck, V. A. Khoze, A. D. Martin, R. Orava and M. G. Ryskin, Eur. Phys. J. C **25** (2002) 391; A. B. Kaidalov, V. A. Khoze, A. D. Martin and M. G. Ryskin, Eur. Phys. J. C **31** (2003) 387.
- [51] J. Bartels, S. Bondarenko, K. Kutak and L. Motyka, Phys. Rev. D **73** (2006) 093004; arXiv:hep-ph/0601128.
- [52] J. Bartels, L. N. Lipatov and M. Wüsthoff, Nucl. Phys. B **464** (1996) 298; G. P. Korchemsky, Nucl. Phys. B **550** (1999) 397; M. A. Braun and G. P. Vacca, Eur. Phys. J. C **6** (1999) 147; R. A. Janik and R. Peschanski, Nucl. Phys. B **549** (1999) 280; J. Bartels, L. N. Lipatov and G. P. Vacca, Nucl. Phys. B **706** (2005) 391.
- [53] R. A. Janik and R. Peschanski, Nucl. Phys. B **565** (2000) 193; J. Polchinski and M. J. Strassler, Phys. Rev. Lett. **88** (2002) 031601; J. Polchinski and M. J. Strassler, JHEP **0305** (2003) 012; G. S. Danilov and L. N. Lipatov, arXiv:hep-ph/0603073; R. C. Brower, J. Polchinski, M. J. Strassler and C. I. Tan, arXiv:hep-th/0603115.
- [54] G. Policastro, D. T. Son and A. O. Starinets, Phys. Rev. Lett. **87** (2001) 081601; P. Kovtun, D. T. Son and A. O. Starinets, Phys. Rev. Lett. **94** (2005) 111601; E. Shuryak, S. J. Sin and I. Zahed, arXiv:hep-th/0511199.
- [55] R. A. Janik and R. Peschanski, Phys. Rev. D **73** (2006) 045013.

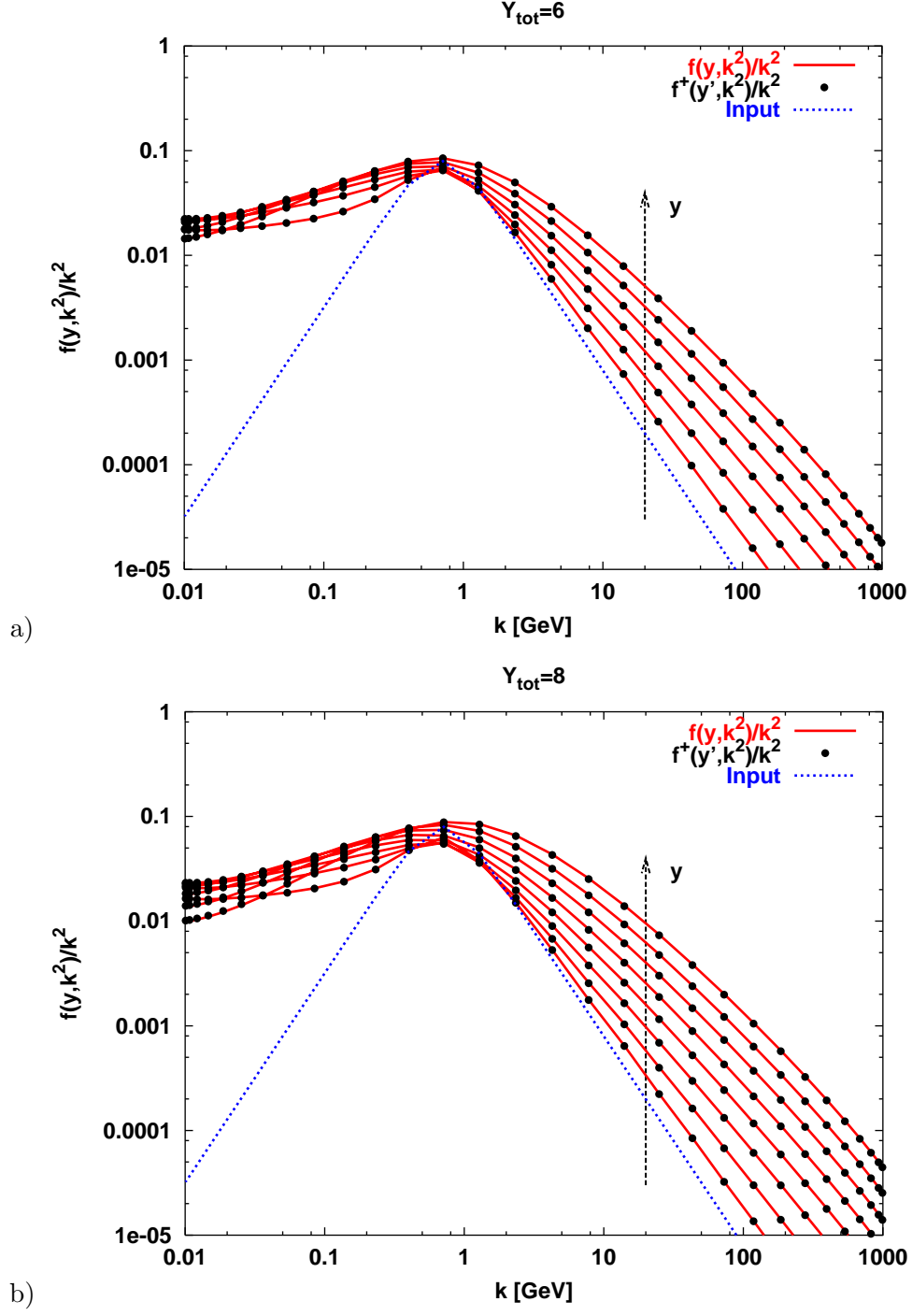


Figure 6: Solutions of the Braun equations $f(y, k^2)/k^2 = f^\dagger(y', k^2)/k^2$ for a) $Y = 6$ and b) $Y = 8$.

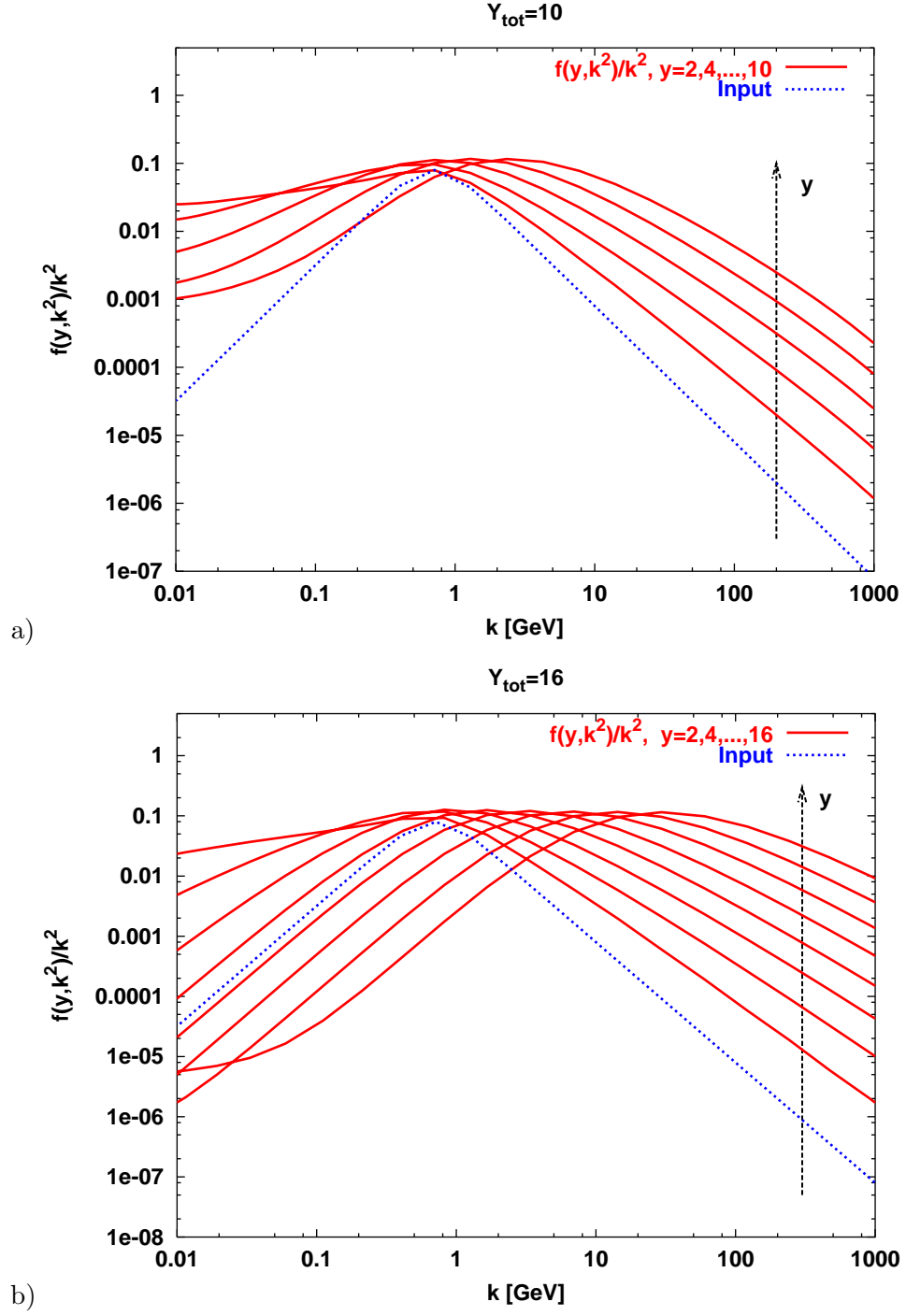


Figure 7: Solutions of the Braun equations $f(y, k^2)/k^2$ for a) $Y = 10$ and b) $Y = 16$.

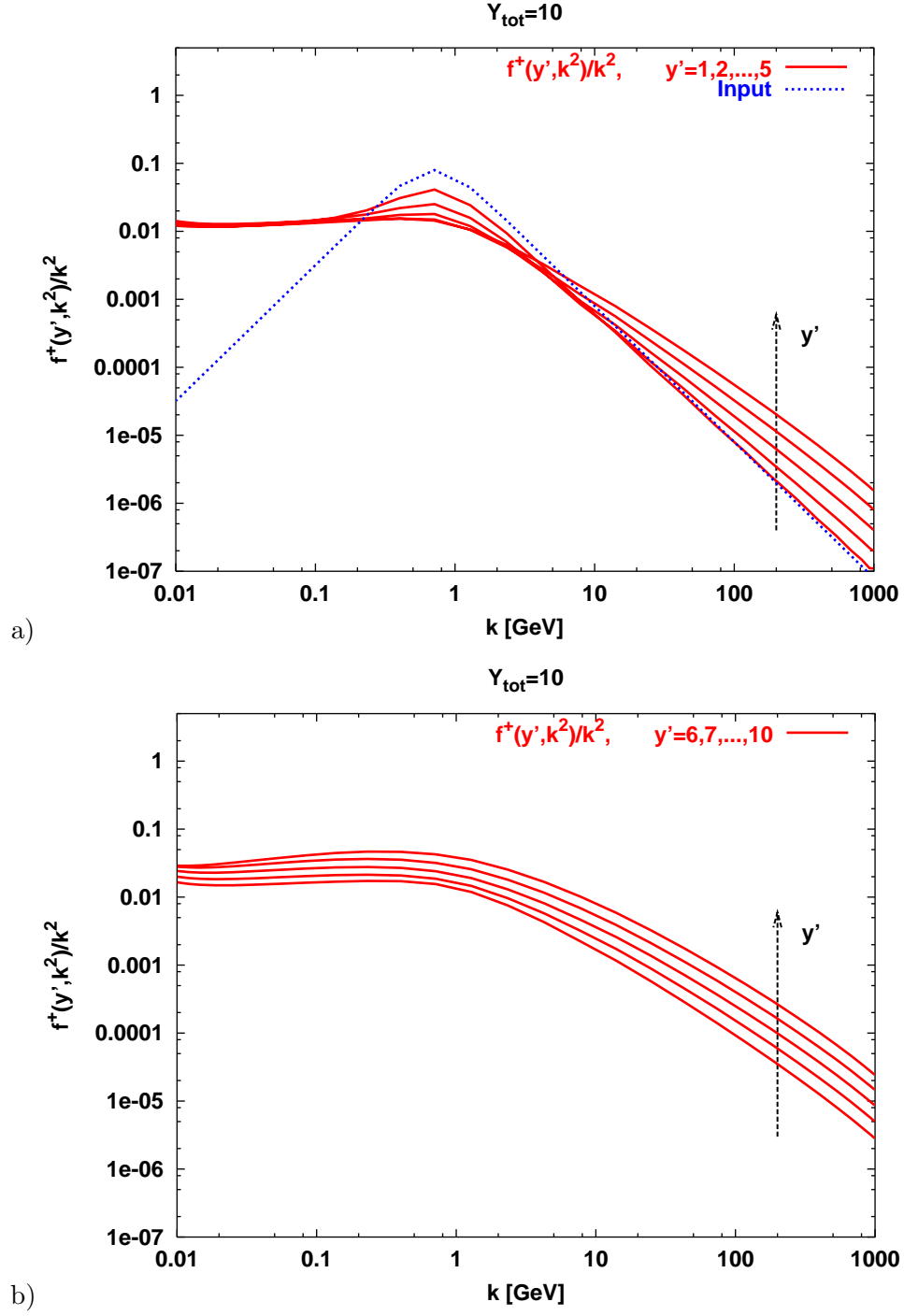


Figure 8: Solutions of the Braun equations $f^+(y', k^2)/k^2$ for $Y = 10$: a) $y' = 0, 1, \dots, 5$; b) $y' = 6, 7, \dots, 10$.

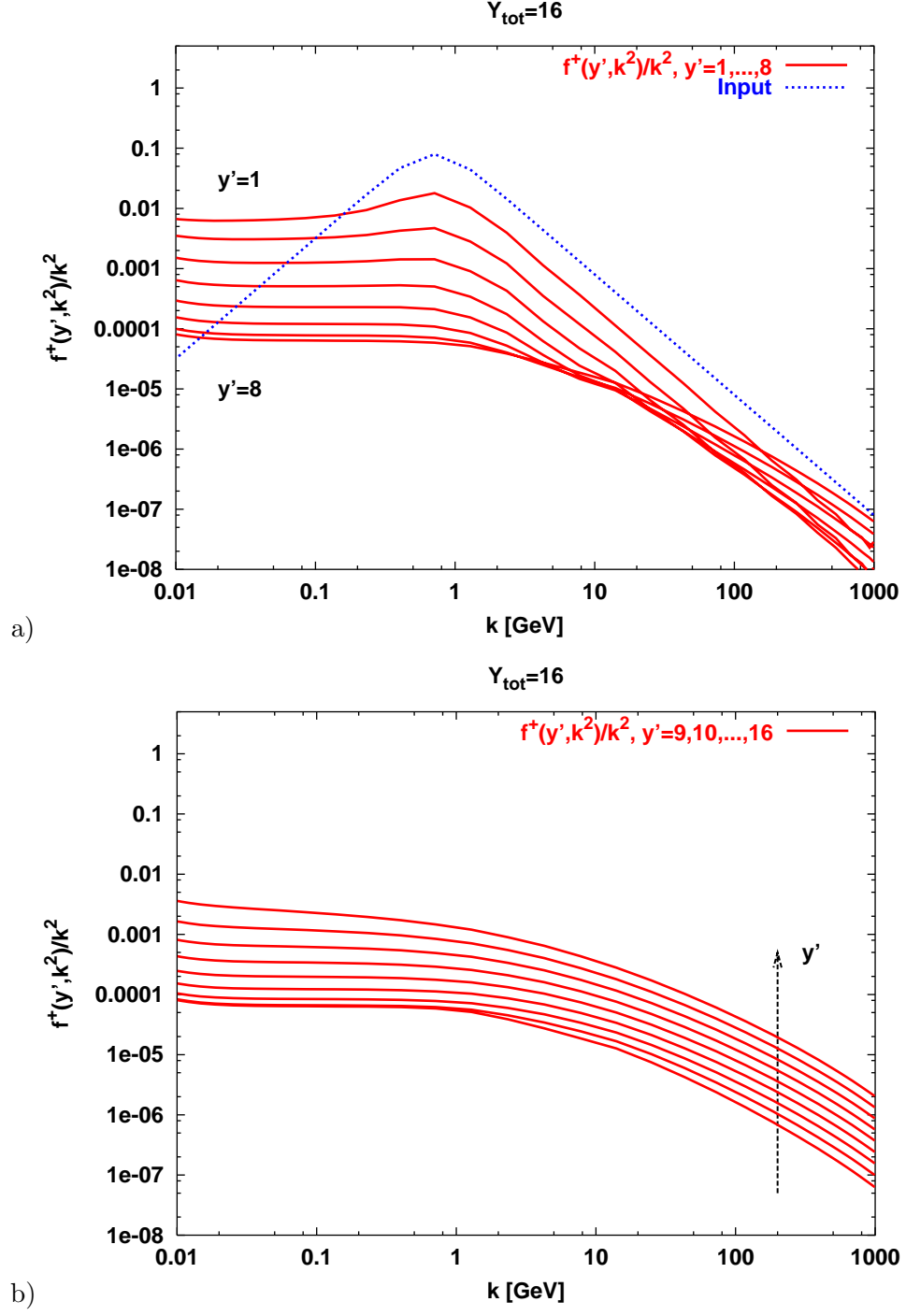


Figure 9: *Solutions of the Braun equations $f^\dagger(y', k^2)/k^2$ for $Y = 16$: a) $y' = 0, 1, \dots, 8$; b) $y' = 9, 10, \dots, 16$.*

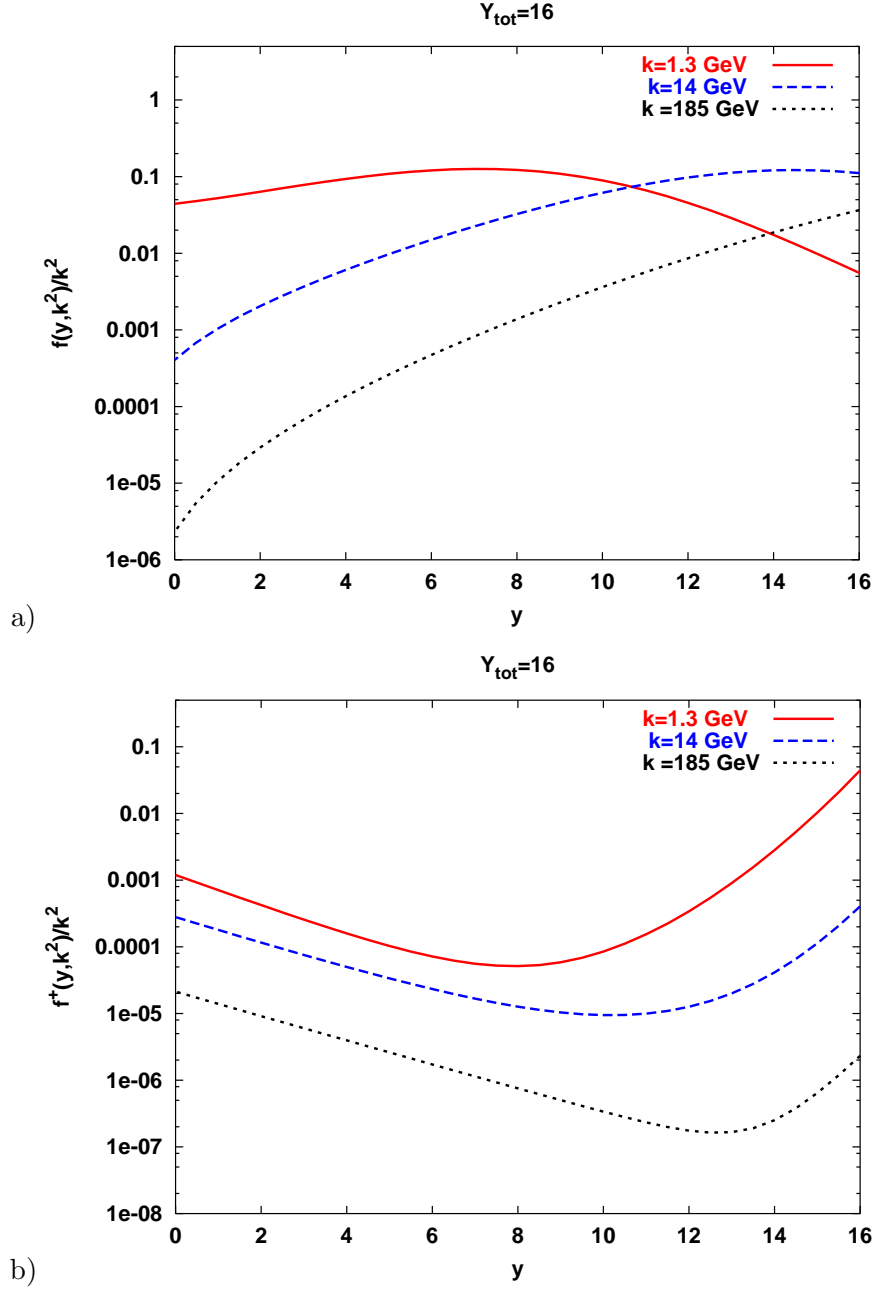
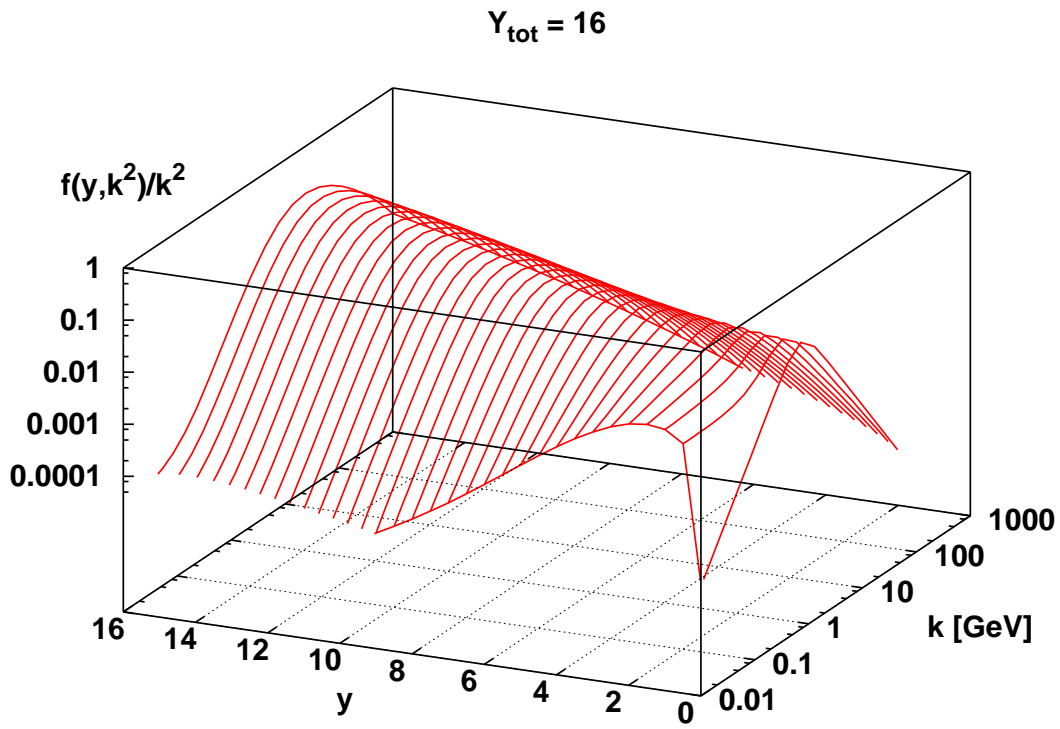
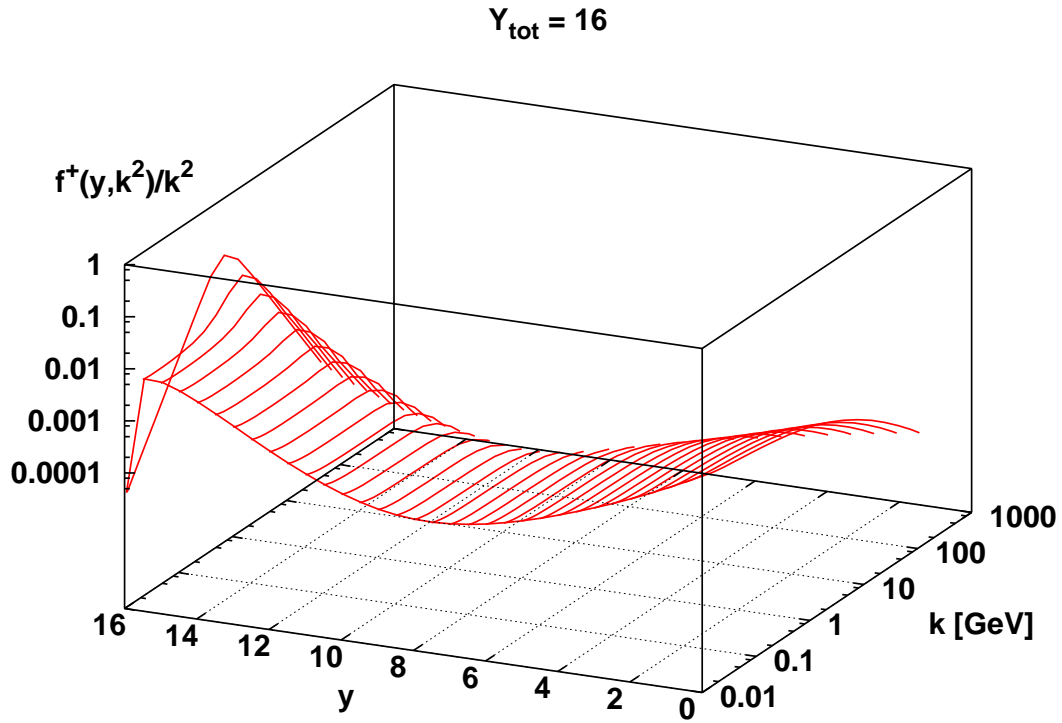


Figure 10: *Solutions of the Braun equations for $Y = 16$ plotted as a function of rapidity y for $k = 1.3$ GeV (solid line), $k = 14$ GeV (dashed line) and $k = 185$ GeV (dotted line): a) $f(y, k^2)/k^2$ and b) $f^+(y, k^2)/k^2$.*



a)



b)

Figure 11: *Solutions of the Braun equations for $Y = 16$ plotted as a function of rapidity y and k : a) $f(y, k^2)/k^2$ and b) $f^+(y, k^2)/k^2$.*

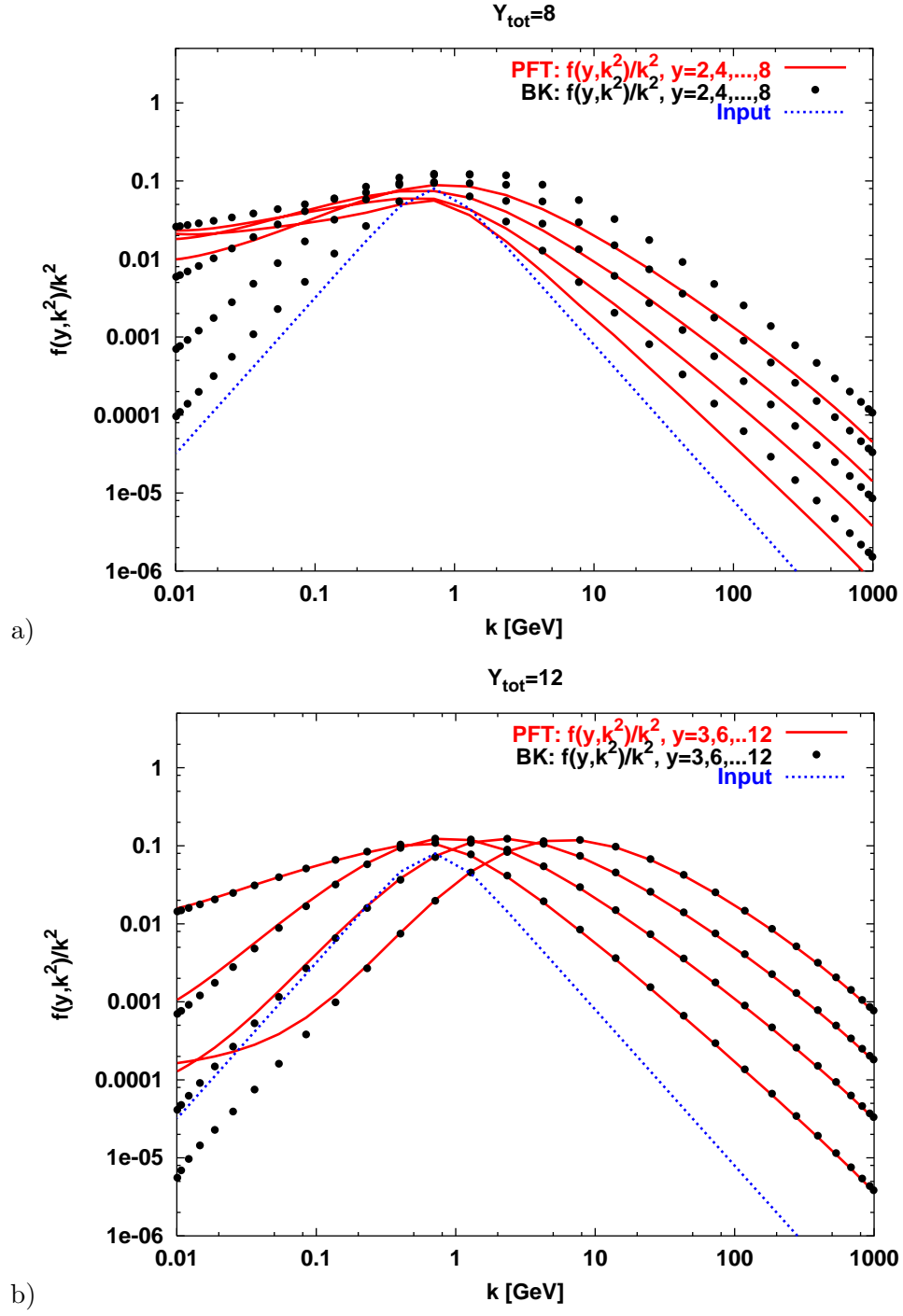


Figure 12: Comparison of the larger solution $f(y, k^2)/k^2$ of the Braun equations (solid line) to the solution of the BK equation (points) for a) $Y = 8$ and b) $Y = 12$.

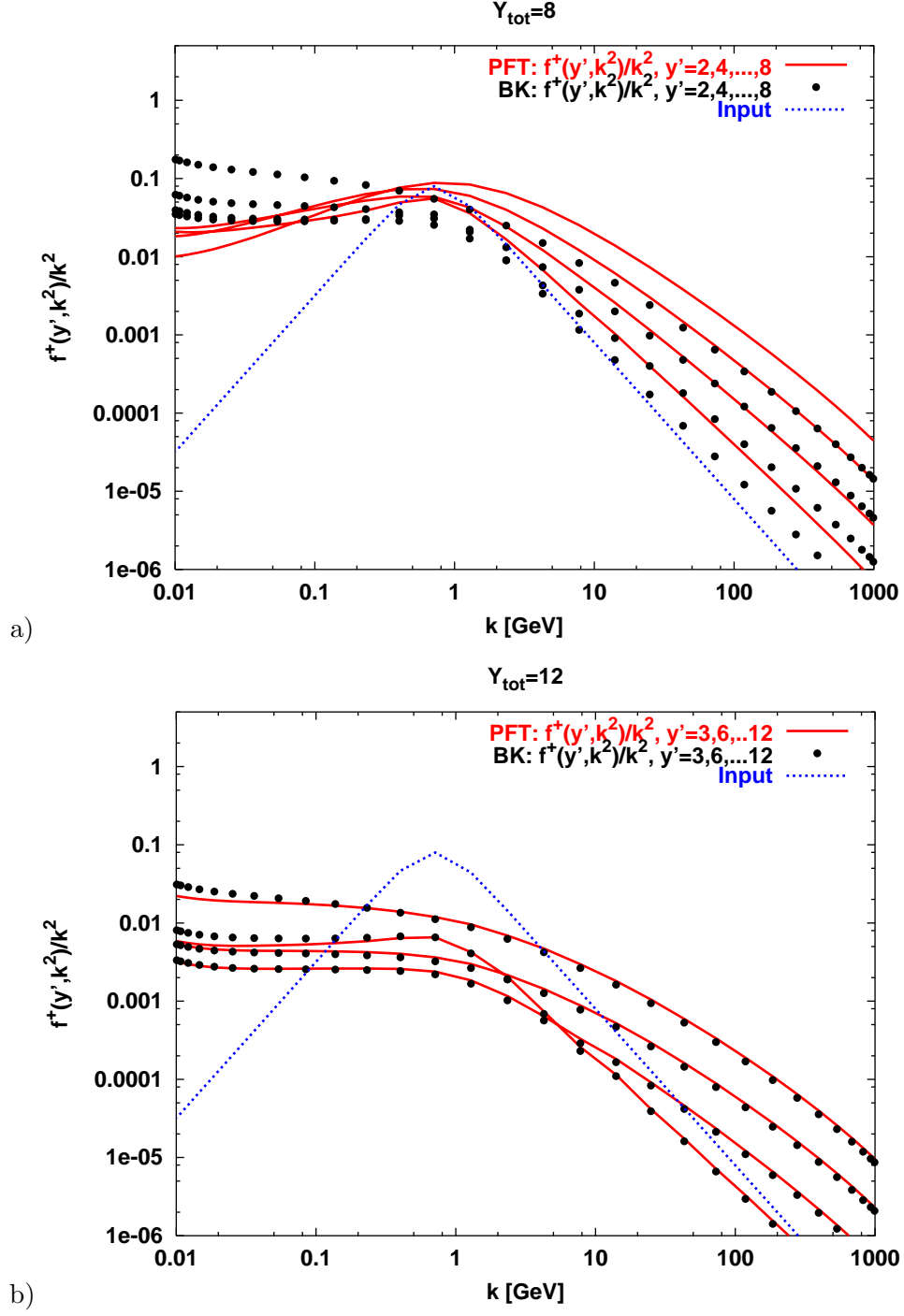


Figure 13: Comparison of the smaller solution $f^+(y', k^2)/k^2$ of the Braun equations (solid line) to the “smaller solution” $f^{\text{BK}}(y', k^2)/k^2$ of the BK equation (points) for a) $Y = 8$ and b) $Y = 12$.

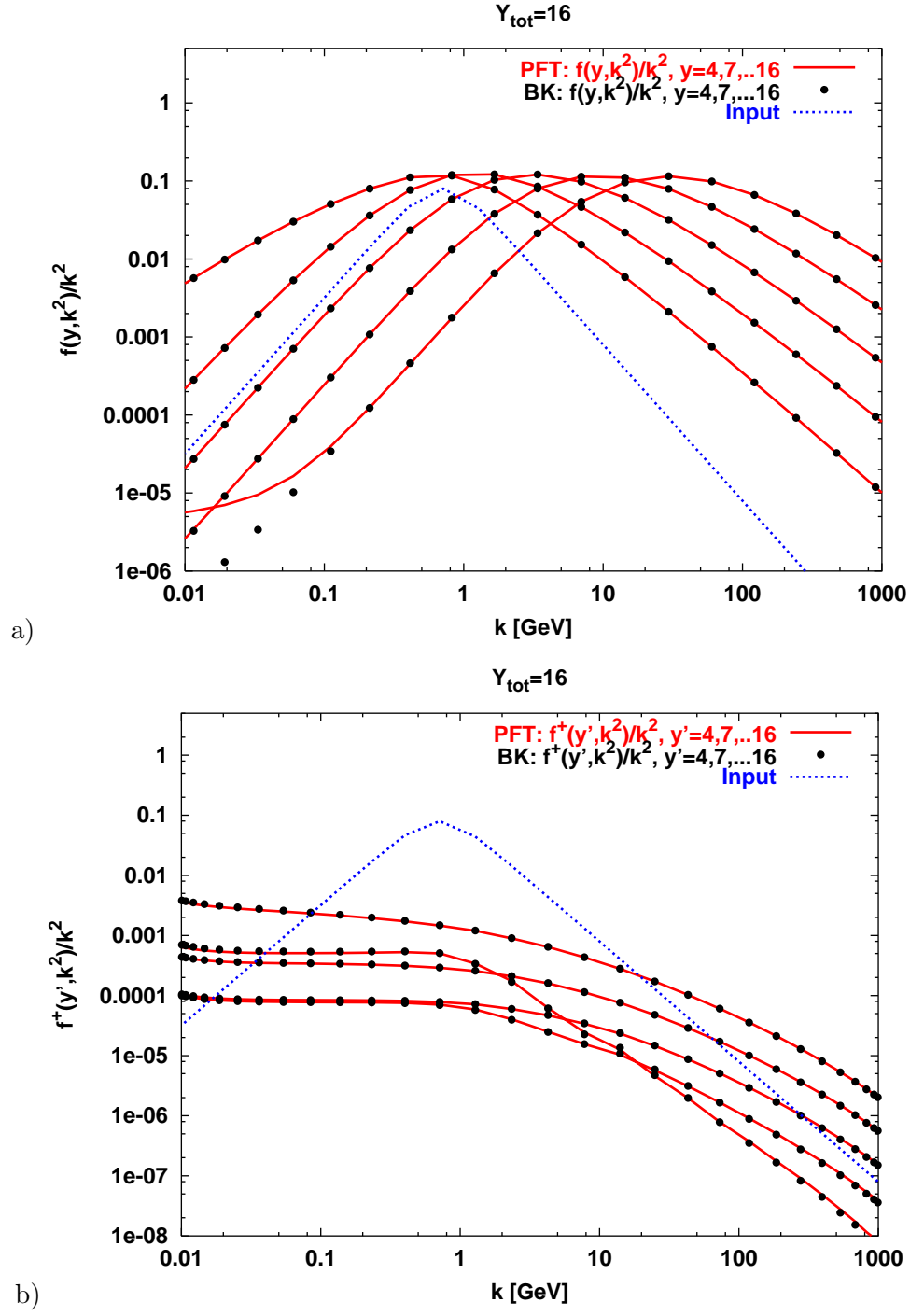


Figure 14: Comparison of the solution of the Braun equations (solid line) to the solution of the BK equation (points) for $Y = 16$: a) the larger solution $f(y, k^2)/k^2$ and b) the smaller solution $f^+(y', k^2)/k^2$.